Coordination Chemistry Reviews, 36 (1981) 267—324
Elsevier Scientific Publishing Company, Amsterdam — Printed in The Netherlands

THE STEREOCHEMISTRY AND ELECTRONIC PROPERTIES OF FLUXIONAL SIX-COORDINATE COPPER(II) COMPLEXES

BRIAN HATHAWAY, MARY DUGGAN, ANGELA MURPHY, JOHN MULLANE, CHRIS POWER, ANDREW WALSH and BERNADETTE WALSH

The Chemistry Department, University College, Cork (Eire)

(First received 4 February 1980; in revised form 23 October 1980)

CONTENTS

ABBREVIATIONS

en	ethylenediamine
bipy	2,2′-bipyridyl
phen	1,10-phenanthroline
dien	diethylenetriamine
ompha	octamethylpyrophosphoramide
H_2edta	ethylenediamine tetraacetic acid dianion

$HBpy_3$	hydro[tris(pyrazol-1-yl)borate] anion
hfacac	hexafluoroacetylacetonate anion
bipyam	2,2′-bipyridylamine
IPCP	tetraisopropylmethylenediphosphorate
fomp	4-formyl-2-methoxyphenolate
meen	*N*,*N*′, *N*″, *N*‴-tetramethylethylenediamine
CAT	1,3-propanediammonium cation
terpy	terpyridine
py	pyridine
TMSO	tetramethylenesulphoxide
NMIz	N-methylimidazole
HDAZ	hexaimidazole
tach	*cis*, *cis*-1,3,5-triaminocyclohexane
PyNO	pyridine-*N*-oxide
thch	trihydroxycyclohexane

A. INTRODUCTION

The copper(II) ion is a typical transition metal ion in that it readily forms stable complexes [1]; it is less typical in the formation of a wide range of stereochemistries [2,3] and in the formation of series of distorted stereochemistries within a given coordination number, especially five and six coordination [4,5]. Despite this complicated behaviour, the relationship between these various stereochemistries and the underlying one-electron orbital levels (and their variation with the distortion present) has been reasonably established using the single-crystal techniques of polarised electronic and electron spin resonance spectroscopy [2,3,6—13]. In nearly all the literature in this field it has been assumed that the stereochemistry determined by single-crystal X-ray crystallography has involved a static stereochemistry of the CuL_n chromophore present. In the great majority of cases this is indeed the case, especially when stereochemistries of extreme tetragonal distortion are involved, such as the square or rhombic coplanar and tetrahedral stereochemistries. Nevertheless, for five and six coordinate complexes there is evidence that not only do the stereochemistries vary over an appreciable range of distortion [4,5] (the plasticity effect, [5]), but there is increasing evidence that the electronic properties of the copper(II) ion in particular six coordinate complexes vary with temperature (especially the ESR spectra) [12,13], which suggests that the underlying stereochemistry of the copper(II) ion is also temperature variable and consequently the room temperature X-ray crystal structure may be perfectly valid, but only relevant to that particular temperature. Consequently for these temperature-variable or fluxional systems [14] it is essential that not only the electronic properties but also the crystal structure should be determined at more than one temperature in order to present an accurate description of the stereochemistry of the copper(II) ion. Only a limited number of X-ray crystal structures of copper-

(II) complexes have been determined at both room temperature and at the temperature of liquid nitrogen and while these are most important they represent only the tip of the iceberg in the saga of fluxional copper(II) complexes. The purpose of this review is (i) to summarise the theoretical model that accounts for the occurrence of fluxional six coordinate copper(II) complexes, (ii) to collect together the structural evidence for fluxional behaviour and to correlate this with the temperature variable electronic properties and (iii) to examine the use of the electronic properties of fluxional * copper(II) complexes in predicting the local CuL_6 chromophore stereochemistry, particularly, that of the compressed tetragonal ** octahedral stereochemistry of copper(II) complexes.

B. THE JAHN-TELLER THEOREM

The origin of the temperature variable stereochemistry for six coordinate complexes of the copper(II) ion lies in the special properties of the [Ar] $3d^9$ electron configuration of the copper(II) ion in an octahedral crystal field, which generates a ^2E_g doubly degenerate ground state [2,3,9]. This ground state is subject to the Jahn-Teller theorem [15] which states that, "if a molecule has an orbital degeneracy when the nuclei are in a symmetrical configuration, then the molecule is unstable with respect to at least one asymmetric distortion of the nuclei and the molecule will distort to lower its energy and remove the orbital degeneracy". The theorem says nothing about the extent of the distortion nor its direction, but in practice [16] the vast majority of six coordinate copper(II) complexes involve an elongated tetragonal octahedral stereochemistry with tetragonalities *** of 0.8—0.85 (the extent of which is usually determined by crystal packing forces [2] such as hydrogen bonding and Van der Waals forces), and involve for all practical purposes static copper(II) stereochemistries. However, for a few six coordinate copper(II) systems with tetragonalities in the region of 0.85—1.0, including the ten complexes described in section C, a more detailed examination of the Jahn-Teller effect and its consequences is required. For a detailed account of this the reader is referred to the excellent reviews [15—24] in the literature.

---

* In this review the term "fluxional" is used to cover the whole range of temperature variable CuL_6 stereochemistries. The term "dynamic Jahn-Teller effect" will be restricted to high symmetry systems, such as octahedral or trigonal octahedral, which generate an orbitally degenerate ground state E_g or E_1 respectively, and the term "pseudo-dynamic Jahn-Teller effect" will be used to describe the properties of low symmetry CuL_6 chromophores whose fluxional properties may be considered to originate from the parent Jahn-Teller effect.

** The term "elongated tetragonal octahedral" will be used to describe both the elongated rhombic and tetragonal octahedral stereochemistries, except where the difference is significant.

*** Tetragonality [2,3], T = mean inplane Cu—L distance/mean out-of-plane Cu—L distance.

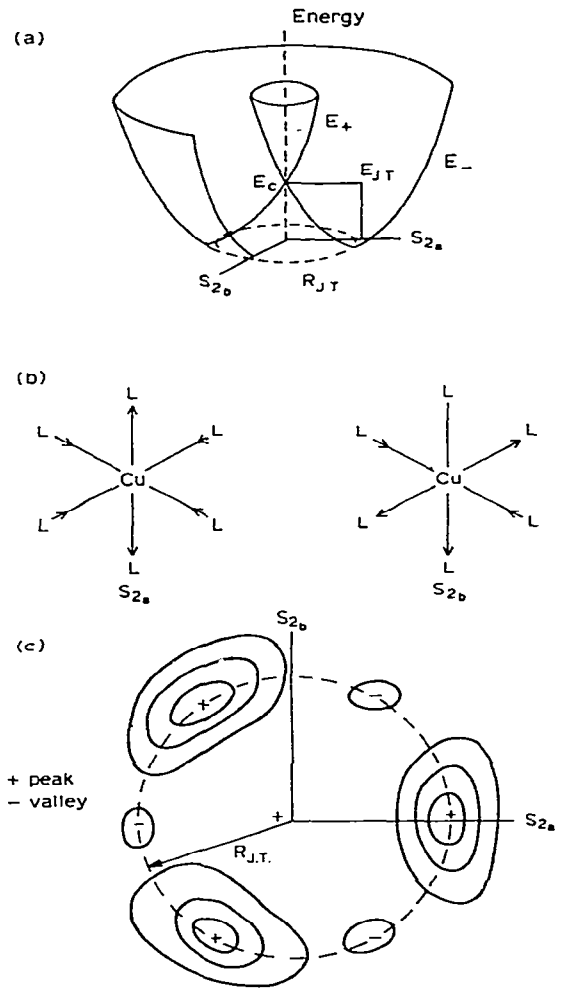

Fig. 1. (a) The potential energy surface (Mexican Hat); (b) the normal coordinates S_{2a} and S_{2b}; (c) the projection of the potential energy surface (a) warped by the inclusion of non-linear terms viewed down the principle axes of (a) with R_{JT} = radius of the minimum potential. Reproduced by permission of the authors [24].

Qualitatively, the electronic properties of the copper(II) ion in these near orbitally degenerate ground states can no longer involve separately defined electronic energies and vibrational energies (the Born-Oppenheimer approximation) but a vibronic potential energy surface, as in Fig. 1(a). The even mode of vibration, of e_g symmetry, made up of two displacement coordinates S_{2a} and S_{2b}, Fig. 1(b), is the only mode that can couple with the electronically degenerate ground state of ^2E_g symmetry, of energy E_0, in a cubic system and remove the orbital degeneracy. The energy surfaces which arise from this

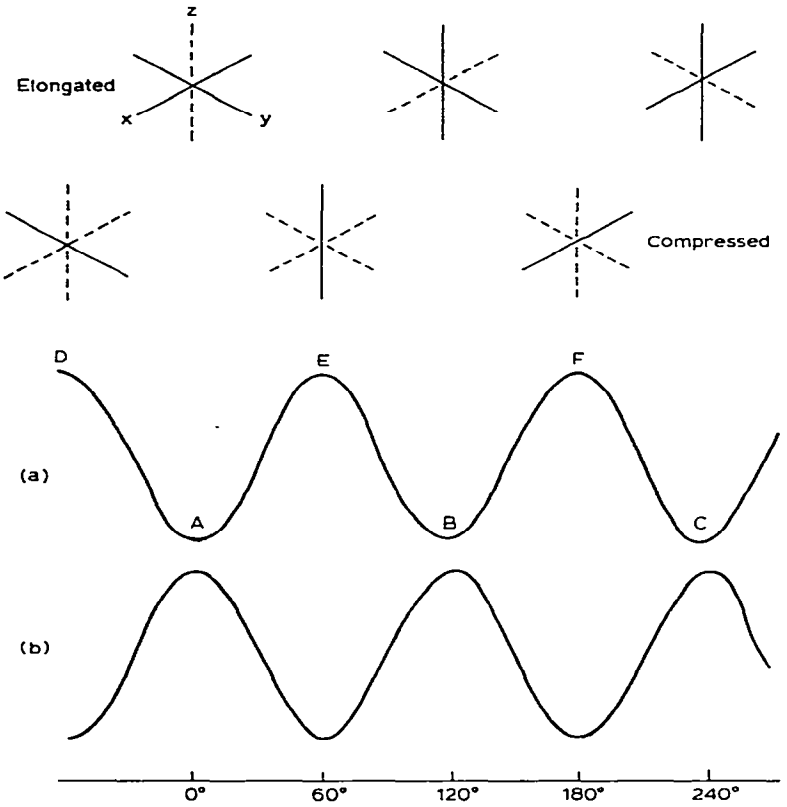

Fig. 2. Circular cross-section of the warping of the potential energy surface minimum E_- for (a) —ve coupling of higher order terms and (b) +ve coupling of higher order terms.

coupling, E_- and E_+, take the form shown in Fig. 1(a), which is known as the "Mexican Hat" model. The surface E_- involves a potential energy minimum, E_{JT}, the Jahn-Teller stabilisation energy, relative to E_0, at a distance R_{JT}, the Jahn-Teller radius, from the origin. If only first order coupling terms are involved the potential energy well has full cylindrical symmetry, but if higher order terms are involved the lower energy surface is warped; if the sign of the coupling constant is negative, Fig. 2(a), minima occur in the potential surface for $\theta = 0$, 120 and 240° and these values correspond at equilibrium to three equivalent elongated tetragonal octahedral distortions, along the three orthogonal directions, z, x and y axes, respectively (Fig. 2(a), points A, B and C). The intermediate higher energy saddles D, E and F where $\theta = 300$, 60 and 180° then correspond at equilibrium to three compressed tetragonal octahedral distortions with the compression along the y, z and x axes respectively, Fig. 2(a). If the sign of the coupling constant is positive then the positions of the elongations and compressions remain the same but their relative energies

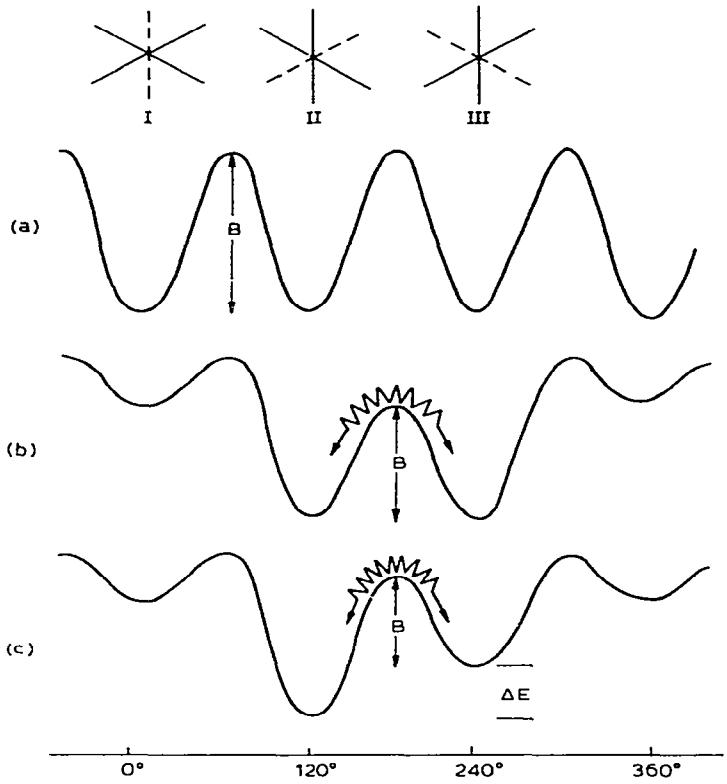

Fig. 3. The circular cross-section of the warped potential energy surface for (a) three Wells of equal energy; (b) two Wells of equal low energy and (c) one low energy Well. Reproduced by permission of the authors [101].

are inverted (Fig. 2(b)). As long as the coupling is restricted to cubic and quadratic terms the overall symmetry of the potential energy surface is still C_{3v}, but with strong Jahn-Teller coupling higher order terms must be included which further warp the potential energy surface such that the strict C_{3v} symmetry is removed. Figure 3 illustrates the three different situations that can arise if three elongated tetragonal octahedral stereochemistries are involved: type (A), all three wells are of equal energy; type (B), two wells are of equal low energy; and type (C), one low energy well occurs. In all three cases a further classification, (i) and (ii), occurs depending on the relative magnitude of the potential energy barrier B and thermal energy kT, as in Table 1.

In A(i) ($B <$ thermal energy (kT, ca. 200 cm^{-1})) all three wells will be equally occupied and the complex will exhibit apparent octahedral symmetry due to a dynamic distortion between the three elongated tetragonal distortions of the nuclear framework and the complex will display a cubic crystal structure, as in $K_2PbCu(NO_2)_6$ [25,26] and $Tl_2PbCu(NO_2)_6$ [21], at room

TABLE 1

The three potential energy wells: (A) three wells of equal energy; (B) two wells of equal low energy and (C) one low energy well, separated by the potential energy barrier B when, (i) B is less than thermal energy kT and when, (ii) B is greater than kT

Type		No. of lowest wells	Symmetry		CuL_6
A(i)	$B < kT$	3	Cubic or Trigonal	Dynamic	Octahedral
A(ii)	$B > kT$	3		Static disordered	Octahedral
B(i)	$B < kT$	2	Tetragonal	Two dimensional, fluxional	Pseudo-compressed octahedral
B(ii)	$B > kT$	2		Two dimensional, static disordered	Pseudo-compressed tetragonal octahedral
C(i)	$B < kT$	1	No symm.	One dimensional, fluxional	Elongated tetragonal octahedral
C(ii)	$B > kT$	1		One dimensional, static	Elongated tetragonal octahedral

temperature. This situation also applies to trigonal tris(chelate)copper(II) complexes such as $Cu(en)_3SO_4$ [27] and $Cu(ompha)_3(ClO_4)_2$ [22], which both crystallise in high symmetry trigonal lattices. In A(ii) ($B >$ thermal energy (kT)) an equal mixture is involved of the three elongated tetragonal octahedral chromophores of Fig. 3(a), with their elongation axes misaligned in three mutually perpendicular directions, with each well (I—III) thermally isolated; the crystal system could still be cubic (or trigonal) with disordered octahedral CuL_6 chromophores, but no definite examples of this situation in concentrated copper(II) complexes are known. For crystals of lower than cubic or trigonal symmetry further warping occurs, and for the situation illustrated in Fig. 3(b), Well I is of considerably higher energy than Wells II and III, which are of approximately equal energy and hence are approximately equally occupied. For B(i) ($B <$ thermal energy (kT)), the two 90° misaligned CuL_6 chromophores are thermally accessible and at any one copper site a two dimensional interconversion of the elongation axes occurs; if the thermal population of Wells II and III are approximately equal the crystallographically determined CuL_6 stereochemistry will appear compressed octahedral, but is better described as pseudo compressed [28] in view of the two dimensional pseudo-dynamic behaviour involved. For B(ii) ($B >$ thermal energy (kT)), then at any one crystallographic site there will be two identical elongated tetragonal octahedral CuL_6 chromophores, which only differ in the

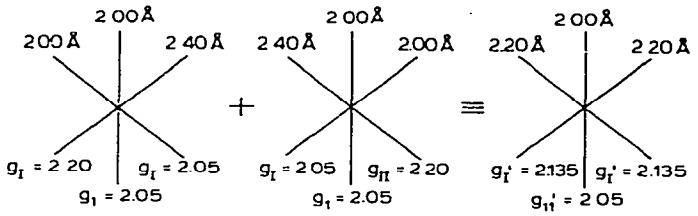

Fig. 4. The effect of two elongated tetragonal octahedral CuL_6 chromophores misaligned by 90° (antiferrodistortive order) on the average Cu—L bond distances and the *g*-factors.

relative orientation of their elongation axes by 90°, as represented in the top half of Fig. 4. With approximately 50% occupancy, the average chromophore stereochemistry will appear to be compressed octahedral, but as this is not a genuine static copper(II) stereochemistry this structural situation is also better referred to as pseudo compressed tetragonal octahedral * or disordered compressed to distinguish it from two dimensional dynamic, B(i), above.

Unfortunately the measurement of the Cu—L bond distances in both situations (B)(i) and (B)(ii) above, will only indicate a time averaged, (i), or a statistically averaged, (ii), pseudo compressed octahedral geometry for the

* This structural situation should not be confused with the structural situation in which the 90° misaligned elongated tetragonal octahedra (Fig. 5(b)) are present at adjacent copper positions as in the lattice [37] of $[CAT]_2CuCl_4$, Fig. 5(d), which involves a slightly distorted two dimensional layering of elongated tetragonal octahedral $CuCl_6$ chromophores, but the different orientations are related by the elements of symmetry of the space group *Pmma* and are not crystallographically distinguishable, a structural situation that is referred to as antiferrodistortive ordering [38].

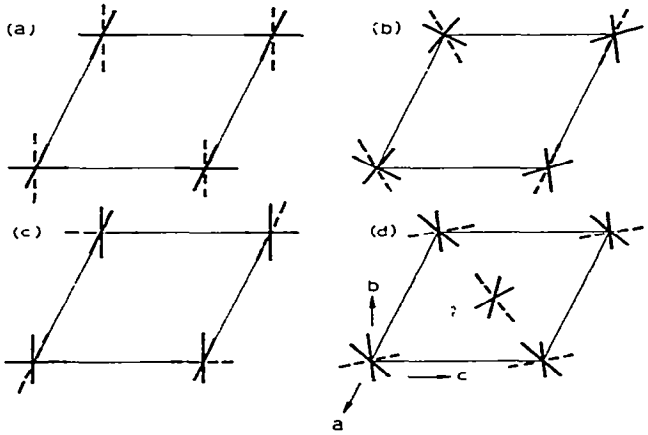

Fig. 5. The types of crystallographical CuL_6 chromophore orientations: (a) aligned (ferrodistortive order); (b) misaligned ($2\gamma \approx 45°$); (c) 90° misaligned (antiferrodistortive order; $2\gamma = 90°$); (d) $[CAT]_2CuCl_4$ (where 2γ = angle between the elongation axes).

CuL_6 chromophore and cannot distinguish directly between these two alternatives. The observed compressed rhombic octahedral geometries of the CuL_6 chromophores of the room temperature structures of $Rb_2PbCu(NO_2)_6$ [29], $Cs_2PbCu(NO_2)_6$ (I) [30], $Cu(dien)_2(NO_3)_2$ (II) [31,32], K_2CuF_4 [33] and Ba_2CuF_6 [34] and the low temperature structures of $K_2PbCu(NO_2)_6$ (III)

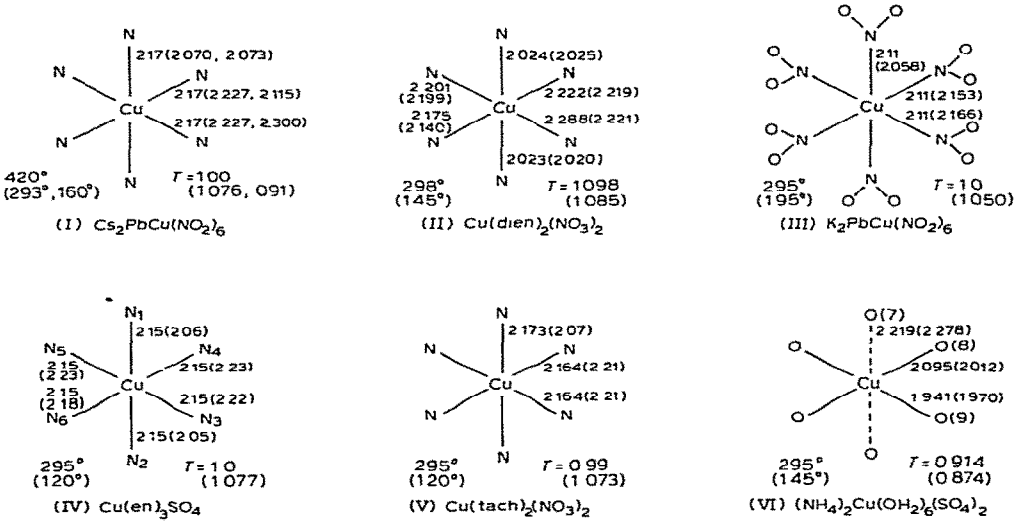

[28], $Cu(en)_3SO_4$ (IV) [35], $Cu(dien)_2(NO_3)_2$ (II) [32] and $Cu(tach)_2(NO_3)_2$ (V) [36] are all believed to involve one or other of the two situations (B)(i) or (B)(ii) above and hence these geometries are best described as pseudo compressed rhombic octahedral [28] (see later).

If the potential energies of Wells II and III are significantly different, (see Fig. 3(c)), then in type (C)(i) ($B <$ thermal energy (kT)), the observed structure will be elongated tetragonal octahedral, but the observed tetragonality will be temperature dependent, precisely as observed in the fluxional stereochemistries of $(NH_4)_2Cu(OH_2)_6(SO_4)_2$ (VI) [39] and $Cu(tach)_2(NO_3)_2$ [40] (V) (section C). In type (C)(ii) ($B >$ thermal energy (kT)), the potential energies of Wells II and III, ΔE, are well separated, the elongated tetragonal octahedral structure of Well II, Fig. 3(c), predominates and the static non-temperature variable elongated tetragonal octahedral stereochemistry occurs as found for the majority of elongated tetragonal octahedral complexes of the copper(II) ion, with tetragonalities in the region $T = 0.80$—0.85 [2,3].

Thus the three diagrams of Fig. 3(a)—(c) contain all the structural situations required to account for the temperature variable stereochemistries described in section C, all of which can be described in terms of one or more elongated tetragonal octahedral CuL_6 chromophores, combined through a vibronic coupling mechanism to describe not only octahedral and elongated tetragonal octahedral chromophore stereochemistries, but even the pseudo compressed tetragonal octahedral as well. The latter could theoretically [41—43] exist in its own right, Fig. 3(b), but at the present time there is no clear

evidence that this stereochemistry can occur in concentrated copper(II) complexes (see section H).

The three types of behaviour depicted in Fig. 3(a)—(c), also have implications in respect to the phase changes [13] involved in transitions between the three types. Type (A) are high symmetry cubic or trigonal, type (B) are generally orthorhombic or tetragonal but can be triclinic, and type (C) are generally low symmetry monoclinic or triclinic. As the three types of behaviour are temperature dependent and determined by the relative magnitude of the potential energy barrier B and thermal energy, lowering the temperature can result in a change in the type of behaviour observed and a possible change in phase [13]. The temperatures of the phase changes give no chemical information, but they are important for all of these dynamic → static systems involving transition from a high to a low symmetry lattice, as this must involve the appearance of a mosaic structure [28,44] at the low temperature, which will result in a varying degree of crystal twinning in the low temperature X-ray structure work. In the low temperature work on both $K_2PbCu(NO_2)_6$ (III) [28] and $Cu(ompha)_3(ClO_4)_2$ (VII) [44] the existence of more than one phase was always a problem, but although solvable in the case of $K_2PbCu(NO_2)_6$ (IIIL) [28] and $Cu(en)_3SO_4$ (IVL) [35] complexes, it was deemed to be too serious a problem to justify the publication of the low temperature crystal structure of $Cu(ompha)_3(ClO_4)_2$ (VII) [44]. In the low temperature crystal structure [32] of $Cu(dien)_2(NO_3)_2$ (II) at ca. 150 K, no change in phase occurred and hence no change in space group $P2_12_12_1$ or

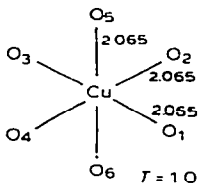

(VII) $Cu(ompha)_3(ClO_4)_2$

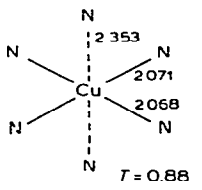

(VIII) $Cu(tach)_2(ClO_4)_2$

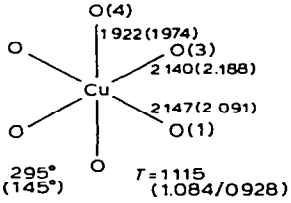

(IX) (methoxyacetate)$_2$·2 H_2O

local molecular structure. Likewise in the low temperature structures of $(NH_4)_2Cu(OH_2)_6(SO_4)_2$ (VI) [39,45], $Cu(tach)_2(ClO_4)_2$ (VIII) [46] and Cu(methoxyacetate)$_2$ · 2 H_2O (IX) [47], no change in phase or space group occurs over this temperature range, and there is only a gradual change in the actual geometry (see section C).

The above model for the effect of the Jahn-Teller theorem on six coordinate copper(II) stereochemistry, has the added advantage of defining the relationship between chromophores with a static stereochemistry and those with a temperature variable or fluxional [14] stereochemistry. It also predicts the order of magnitude of some of the parameters [24] involved and the type of physical techniques that might be used to measure these quantitatively. The Jahn-Teller radius $R_{JT} \approx 0.3$ Å is available from X-ray diffraction data, the angular barrier height $B \approx 100$—1000 cm^{-1} is available from electron spin resonance measurements and the Jahn-Teller energy $E_{JT} \approx 2000$ cm^{-1} can be

examined by optical spectroscopy. The following sections will examine the information available from these three techniques to determine their usefulness in predicting the presence of fluxional properties in copper(II) complexes.

C. LOW TEMPERATURE X-RAY CRYSTALLOGRAPHIC DATA

(i) $K_2PbCu(NO_3)_6$

The most interesting structure is that of $K_2PbCu(NO_2)_6$ (III) which is cubic at room temperature [25,26], space group $Fm3$, with the copper(II) atom occupying a regular octahedral stereochemistry with a Cu—N bond distance of 2.118 Å; below room temperature [28], 276 K, the space group changes to orthorhombic and the local molecular stereochemistry to compressed rhombic octahedral which does not change significantly down to 193 K [28], Table 2. The corresponding tetragonalities change from 1.0 at room temperature to 1.049 and 1.034 for the two low temperature structures, values which compare with those observed in the corresponding room temperature structures of $Rb_2PbCu(NO_2)_6$ (XI) [29], and $Cs_2PbCu(NO_2)_6$ (I) [30], (Table 2) which both involve a compressed rhombic octahedral CuN_6 chromophore

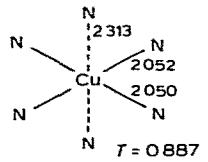

(X) $K_2CaCu(NO_2)_6$

and contrast with those for the elongated rhombic octahedral chromophore of the $K_2CaCu(NO_2)_6$ (X), $K_2SrCu(NO_2)_6$ and $K_2BaCu(NO_2)_6$ complexes (Table 2) [48—50].

(ii) $Cu(en)_3SO_4$

The room temperature crystal structure [27] of $Cu(en)_3SO_4$ (IV) has been solved in the trigonal space group $P\bar{3}1c$, with the copper(II) ion involved in a regular trigonal stereochemistry of D_3 symmetry with Cu—N distances of 2.150 Å. The low temperature structure [35] at 120 K, was solved in the triclinic space group $P\bar{1}$ with very little distortion of the original lattice, a = 8.814(8.966) *; b = 8.896(8.966); c = 9.588(9.597) Å; α = 90.34(90.00); β = 89.73(90.0) and γ = 119.80°(120.0) and Z = 2. The CuN_6 stereochemistry is then best described as compressed rhombic octahedral with a tetragonality of 1.078, rather higher than the low temperature (L) tetragonalities of the $K_2PbCu(NO_2)_6$ (IIIL) complex and the room temperature (R) value for

* Data in parentheses refer to the room temperature data.

TABLE 2

The Cu—N bond distances (Å) in $(M^{I})(M^{II})Cu(NO_2)_6$ complexes

M^{II}	Pb							Ca	Sr	Ba	Pb
M^{I}	K	K	K	Rb	Cs	Cs	Cs	K	K	K	Th
Temp. (K)	295	276	193	295	420	293	160	295	295	295	295
Cu—N(1)	2.118	2.058	2.071	2.063	2.17	2.070	2.073	2.313	2.310	2.311	2.118
Cu—N(2)	2.118	2.153	2.151	2.173	2.17	2.227	2.115	2.052	2.041	2.048	2.118
Cu—N(3)	2.118	2.166	2.133	2.173	2.17	2.227	2.300	2.050	2.029	2.038	2.118
Tetragonality [a]	1.00	1.049	1.034	1.053	1.00	1.076	0.91	0.887	0.881	0.884	1.0

[a] Tetragonality, T = mean inplane Cu—N distance/mean out-of-plane Cu—N distance.

TABLE 3

The Cu—N distances (Å) in $Cu(en)_3SO_4$ (IV)

Bond	Temp. (K)		Disordered		
	295	120	(1)	(2)	(3)
Cu—N(1)	2.15	2.06	2.16	2.16	2.46
Cu—N(2)	2.15	2.05	2.17	2.17	2.34
Cu—N(3)	2.15	2.22	2.04	2.26	2.04
Cu—N(4)	2.15	2.23	2.37	2.08	2.08
Cu—N(5)	2.15	2.23	2.01	2.23	2.01
Cu—N(6)	2.15	2.18	2.44	2.15	2.15
Tetragonality	1.0	1.077	0.871	0.953	0.863

$Rb_2PbCu(NO_2)_6$ of 1.053, but comparable to the room temperature value of $Cs_2PbCu(NO_2)_6$ (I) of 1.077, and to both the room [31] and low [32] temperature structures of $Cu(dien)_2(NO_3)_2$ (II) of 1.098 and 1.085, respectively. The compressed rhombic octahedral CuN_6 chromophore of $Cu(en)_3SO_4$ (IVL) has been analysed as a disordered structure [12,35] involving three elongated rhombic octahedral chromophores (Table 3) whose elongation axes are misaligned by approximately 90° and related by the original three fold axis of the room temperature structure (IVR). The tetragonalities given in columns (1) and (3) are comparable, (0.867), while that of column (2) is significantly higher (0.953).

(iii) $Cu(tach)_2(NO_3)_2$

The CuN_6 chromophore stereochemistry [24] of $Cu(tach)_2(NO_3)_2$ (V) involves six nearly equivalent Cu—N distances (2.164—2.173 Å), despite the involvement of two tridentate nitrogen chelate ligands, with a tripod conformation, yielding six potentially equivalent ligands. The $Cu(tach)_2$ cation has C_{2h} site symmetry and the difference between the two crystallographically different Cu—N distances is not significant; consequently despite the low crystal symmetry the CuN_6 chromophore is considered to undergo a dynamic Jahn-Teller distortion at room temperature [24]. At low temperature [26], ca. 120 K, a compressed tetragonal CuN_6 chromophore is involved with a tetragonality, $T = 1.073$, comparable to the low temperature tetragonalities of 1.078 for $Cu(en)_3SO_4$ (IV) [35] and slightly higher than that of 1.034 for $K_2PbCu(NO_2)_6$ (III) [28].

(iv) $Cu(dien)_2(NO_3)_2$

The crystal structure [31] of $Cu(dien)_2(NO_3)_2$ (II) has been determined at 298 K and ca. 145 K. The CuN_6 chromophore, involving two planar tri-

dentate chelate ligands, has a compressed rhombic octahedral stereochemistry with a tetragonality of 1.098 at room temperature which only decreases slightly to 1.085 at low temperature [32], a difference that is only just significant and primarily associated with the relatively long in-plane Cu—N distance of 2.288 Å in the room temperature structure. In the low temperature structure [32] of $Cu(dien)_2(NO_3)_2$ (II) not only is the compressed rhombic octahedral stereochemistry retained, but the space group $P2_12_12_1$ remains unchanged, a behaviour that parallels the data for the $K_2PbCu(NO_2)_6$ (III) complex [28] between 276 and 195 K (Table 1). Attempts to resolve the CuN_6 chromophore of the room temperature structure (IIR) into two 90° misaligned elongated CuN_6 chromophores (see later) were unsuccessful [31].

(v) Copper Tutton salts

The crystal structure of $(NH_4)_2Cu(OH_2)_6(SO_4)_2$ (VI) has been measured at 295 [51,52], 145 [39,45] and 215 K [45]. The complex crystallises in the monoclinic space group $P2_1/a$, which remains unchanged at all three temperatures, with the copper(II) at a centre of symmetry. At room temperature the structure of the $Cu(OH_2)_6^{2+}$ cation involves an elongated rhombic octahedral stereochemistry with a relatively high tetragonality of 0.914. There are significant changes in two of the Cu—O bond distances with decreasing temperature, the Cu—O(7) distance increases with decreasing temperature, the Cu—O(8) distance decreases and the Cu—O(9) distance shows no significant change. The stereochemistry is elongated rhombic octahedral at all three temperatures but the observed tetragonalities Table 4(a) are significantly less than 1.0 and decrease with decreasing temperature. The tetragonalities of the corresponding potassium [53], rubidium (XI) [54] and caesium [54] Tutton salts, Table 4(b), are much more comparable and similar to the low temperature tetragonalities of the ammonium Tutton salts. Although the differences in the tetragonalities are small, the correlation of tetragonalities with axial bond

TABLE 4

The Cu—OH_2 bond distances of $(NH_4)_2Cu(OH_2)_6(SO_4)_2$ at various temperatures and $(M^I)_2Cu(OH_2)_6(SO_4)_2$ at room temperature and low temperature

Bond	$(NH_4)_2Cu(OH_2)_6(SO_4)_2$					
	295 K	215 K	145 K	M^I = K	M^I = Rb	M^I = Cs
Cu—O(7)	2.219	2.250	2.278	2.069	2.031(2.000) [a]	2.004
Cu—O(8)	2.095	2.041	2.012	2.278	2.307(2.317) [a]	2.315
Cu—O(9)	1.961	1.967	1.970	1.943	1.957(1.978) [a]	1.966
Tetragonality	0.914	0.891	0.874	0.881	0.864(0.858) [a]	0.858

[a] Low temperature data (77 K).

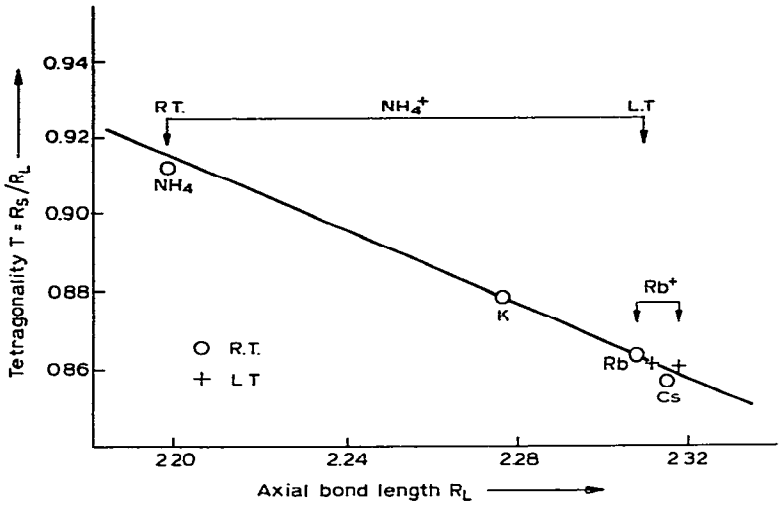

Fig. 6. Copper Tutton salts. Tetragonality vs. axial Cu—O bond length, R_L [31].

length, Fig. 6, does suggest that there is a significant difference between the Tutton salts at room and low temperature. The marked effect of temperature on the ammonium salts contrasts with an almost insignificant temperature effect on the $Rb_2Cu(OH_2)_6(SO_4)_2$ (XI) [55], Table 4(b), and the corre-

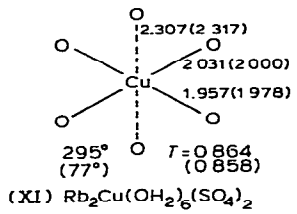

(XI) $Rb_2Cu(OH_2)_6(SO_4)_2$

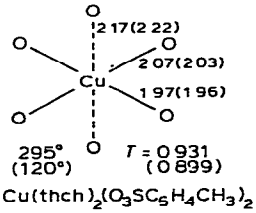

(XII) $Cu(thch)_2(O_3SC_5H_4CH_3)_2$

lation of Fig. 6 suggests [39] that the observed tetragonality is a function of the atomic size of the cation present in this series of Tutton salts. It also establishes [39] the situation that even for the same cationic species, $[Cu(OH_2)_6]^{2+}$, different temperature variations may be present: for the ammonium salt marked temperature variation is present; for the rubidium salt only slight temperature variation is present and for the caesium salt the more usual static stereochemistry is observed, as confirmed by the neutron powder data for α-$Cu(HCO_2)_2$ [56], where $T = 0.756$, 0.758 and 0.762 at 296, 80 and 4 K, respectively, indicating a negligible variation of structure over the range of 292 K.

(vi) $Cu(thch)_2(O_3SC_6H_4CH_3)_2$

The crystal structure of $Cu(thch)_2(O_3SC_6H_4CH_3)_2$ (XII) has been measured at room temperature and at the temperature of liquid nitrogen [46] (where

thch is a tripod type, tridentate ligand). The stereochemistry of the CuN_6 chromophore is elongated rhombic octahedral but with a significant decrease in the observed tetragonality from 0.931 at room temperature to 0.899 at the low temperature, there is a change that parallels that observed in the ammonium Tutton salt.

(vii) $Cu(phen)_3(NO_3)_2 \cdot 2\,H_2O$

The room temperature structure of $Cu(phen)_3(NO_3)_2 \cdot 2\,H_2O$ (XIII) [57] has a clear elongated rhombic octahedral CuN_6 chromophore, which becomes

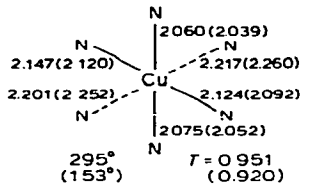

(XIII) $Cu(phen)_3(NO_3)_2 \cdot 2H_2O$

significantly more elongated [58] at 153 K, with the tetragonality decreasing from 0.951 to 0.920 and consistent with a Fig. 3(c) (i) fluxional behaviour.

(viii) $Cu(methoxyacetate)_2 \cdot 2\,H_2O$

The crystal structure [40,47] of $Cu(methoxyacetate)_2 \cdot 2\,H_2O$ (IX) has also been determined at room temperature and at approximately 145 K [47]. At the former temperature the centrosymmetric CuO_6 chromophore, involving two *trans* methoxyacetate chelate ligands and two *trans* water molecules, O(4), involves a compressed rhombic octahedral stereochemistry with close to axial symmetry and a tetragonality of 1.115. At low temperature the tetragonality decreases to 1.084, primarily due to a significant elongation of the inplane Cu—O(3) bond distance from 2.140 Å at room temperature to 2.188 Å at liquid nitrogen temperature. The marked increase (0.048 Å) of the Cu—O(3) bond distance plus the equally significant decrease (0.056 Å) of the Cu—O(1) distance suggest that the low temperature structure might equally be considered as an elongated rhombic octahedral stereochemistry with the elongation along the Cu—O(3) bond direction. Consequently the structure of $Cu(methoxyacetate)_2 \cdot 2\,H_2O$ may be unique in involving a change from a compressed rhombic octahedral stereochemistry at room temperature to an elongated rhombic octahedral stereochemistry at low temperature, with a 90° rotation of the approximate principal axis of the CuO_6 chromophore from the Cu—O(4) direction to the Cu—O(3) direction, a behaviour that is consistent with a transition from a Fig. 3(b)(i) behaviour at room temperature to a Fig. 3(c)(i) behaviour at 145 K. In addition there is also a significant increase (0.05 Å) in the Cu—O(4) distance: consequently the Cu—O bond distance temperature changes, observed in Cu(methoxy-

acetate)$_2$ · 2 H_2O involve a three dimensional change in stereochemistry compared to the two dimensional change observed in the Tutton salts [45].

(ix) $Cs_2PbCu(NO_2)_6$

The system that best illustrates the three types of behaviour predicted by Fig. 3(a)(i)—3(c)(i) is $Cs_2PbCu(NO_2)_6$ (I) [13,30] Table 2, which is cubic at 420 K (α-phase, *Fm*3) [13,30] with an octahedral CuN_6 chromophore; orthorhombic at 323 and 293 K (β- and β'-phase, *Fmmm*) with a pseudo compressed octahedral CuN_6 chromophore; and monoclinic at 160 K (γ-phase, *B*2/*b*) with an elongated rhombic octahedral CuN_6 chromophore. The tetragonality of the pseudo compressed room temperature structure, Fig. 3(b)(i), is 1.077, and that at 160 K is 0.91, Fig. 3(c)(i), suggesting some residual fluxional behaviour, cf. 0.887 for $Cs_2PbCu(NO_2)_6$, Table 2, although too much weight should not be placed on the 160 K structure as this was determined by profile analysis of powder neutron diffraction data.

D. ANISOTROPIC THERMAL PARAMETERS

The presence of a dynamic Jahn-Teller behaviour in the CuL_6 chromophores of these fluxional complexes should be reflected in a marked aniso-

TABLE 5

A comparison of the nitrogen atom thermal motion for $M^I_2M^{II}M(NO_2)_6$ systems; root-mean-square displacements (Å), displacements along the M—N bonds are indicated by an asterisk. Reproduced by permission of the authors [24]

		U_{11}	U_{22}	U_{33}
(a) Non Jahn-Teller complexes				
$K_2PbNi(NO_2)_6$	N(1)	0.130	0.133	0.115*
$K_2SrNi(NO_2)_6$	N(1)	0.120	0.122	0.110*
(b) Static Jahn-Teller complexes				
$K_2SrCu(NO_2)_6$	N(1)	0.141	0.144	0.119*
	N(2)	0.113*	0.121	0.138
	N(3)	0.130	0.111*	0.129
(c) Dynamic Jahn-Teller complexes (cubic)				
$K_2PbCu(NO_2)_6$	N(1)	0.170	0.164	0.182*
(d) Pseudo compressed Jahn-Teller complexes				
$K_2PbCu(NO_2)_6$ (276 K)	N(1)	0.17	0.17	0.11*
	N(2)	0.15	0.16*	0.15
	N(3)	0.18*	0.11	0.25
$Rb_2PbCu(NO_2)_6$	N(1)	0.148	0.152	0.128*
	N(2)	0.182	0.190*	0.141
	N(3)	0.199*	0.151	0.144

tropy in the thermal motions of the six ligand atoms involved. As the differences are only small, care must be taken with the data collection and the data, preferably, corrected for absorption, in order to minimise the effect of any systematic errors in the data. The first evidence for significant thermal motion, as evidence for dynamic Jahn-Teller effects was in the data for Cu(en)$_3$SO$_4$ (IV) [27] and $K_2PbCu(NO_2)_6$ (III) [25], but a wider discussion [24] of the effect for the $M_2^IM^{II}Cu(NO_2)_6$ system has been given involving the comparison of the root-mean-square displacements of the ligand atoms of the non-Jahn-Teller complexes $M_2^IM^{II}Ni(NO_2)_6$, for static $M_2^IM^{II}Cu(NO_2)_6$ (such as $K_2BaCu(NO_2)_6$) and fluxional $M_2^IM^{II}Cu(NO_2)_6$, (such as $K_2PbCu(NO_2)_6$ (III)) at room temperature and at low temperature, Table 5. For nondynamic systems, such as the nickel(II) complexes and the static copper(II) complexes, as the bending modes of an M—ligand bond are of lower energy than the stretching modes, higher root-mean-square displacements will occur perpendicular to the M—ligand bond directions, than along them, as shown in Table 5(a) and (b). For dynamic Jahn-Teller systems the opposite will apply (Table 5(c)) and for the pseudo compressed Jahn-Teller systems (Table 5(d)) which involve a static distortion along Cu—N(1), but a dynamic distortion along Cu—N(2) and Cu—N(3), smaller root-mean-square displacements are predicted to lie along the Cu—N bonds for N(1), but larger root-mean-square displacements for N(2) and N(3). These predictions are clearly born out for $Rb_2PbCu(NO_2)_6$, but only partially for the less accurate data for $K_2PbCu(NO_2)_6$ (III) (276 K).

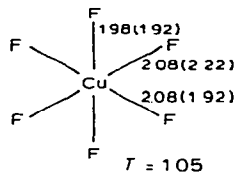

(XIV) K_2CuF_4

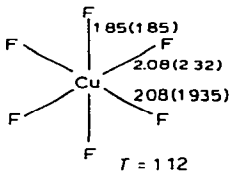

(XV) Ba_2CuF_6

Similar conclusions from the anisotropic temperature factors of the room temperature structures of K_2CuF_4 (XIV) [3] and Ba_2CuF_6 (XV) [34] also

TABLE 6

Some $\Delta U^{1/2}$ (Cu—ligand) (Å) for $Cu(NO_2)_6^{4-}$ chromophores. Reproduced by permission of the authors [24]

Compound	N(1)	N(2)	N(3)
(a) Dynamic			
$K_2PbCu(NO_2)_6$	0.144	0.144	0.144
$Rb_2PbCu(NO_2)_6$	0.062 (static)	0.145	0.147
(b) Static			
$K_2PbNi(NO_2)_6$	0.047	0.047	0.047
$K_2SrCu(NO_2)_6$	—0.030	0.040	0.053

TABLE 7

Some $\Delta U^{1/2}$ (Cu—ligand) (Å) values for some CuL_6 (and NiL_6) chromophores. Reproduced by permission of the author [60]

Compound	L(1)	L(2)	L(3)
$Cu(en)_3(SO_4)$	0.176		
$Ni(en)_3(SO_4)$	0.097		
$Cu(tach)_2(ClO_4)_2$	0.095	0.136	0.151
$Cu(tach)_2(NO_3)_2$	0.147	0.143	0.143
$Ni(tach)_2(NO_3)_2$	0.052	0.052	—
$Cu(dien)_2(NO_3)_2$	0.248	0.063	0.186
Cu(trispyrazolborate)$_2$ (1)	0.07	0.04	<0.00
(2)	0.15	0.12	0.07
$(NH_4)_2Cu(OH_2)_6(SO_4)_2$	0.125	0.115	0.036
Cu(methoxyacetate)$_2 \cdot 2\ H_2O$	0.102	0.097	0.118

suggest that the compressed stereochemistry is better described as due to antiferrodistortive order [59,60], a type of disorder which is also consistent with the observed anisotropies of the root-mean-square displacements, but cannot distinguish this from a two dimensional Jahn-Teller effect or static disorder.

The analysis of the root-mean-square displacements for CuL_6 chromophores in low symmetry systems can also be indicative of fluxional behaviour, but has been expressed [24] in the form $\Delta U^{1/2}$[Cu—N(1)] (Table 6) where the nitrogen displacements are corrected for the displacements of the copper atom and the ΔU values represent a bond displacement, rather than an isolated ligand atom displacement, directed along the Cu—ligand directions. Using this analysis for the $M_2^{I}M^{II}Cu(NO_2)_6$ systems of Table 5, identical conclusions in respect of a static or dynamic behaviour are deduced, the $\Delta U^{1/2}$(Cu—N) values for static systems are <0.05 Å, while for dynamic systems the values are >0.10 Å (Table 6). Using the $\Delta U^{1/2}$(Cu—ligand) values (Table 7) and the above criteria, this suggests that $Cu(en)_3SO_4$ (IV) [27] involves a genuine dynamic Jahn-Teller effect, that $Cu(tach)_2(NO_3)_2$ (V) [24] is as near a dynamic system as a CuN_6 chromophore in a low symmetry lattice can be, and that the CuN_6 chromophore of $Cu(tach)_2(ClO_4)_2$ (VIII) [24] and $Cu(dien)_2(NO_3)_2$ (II) [31], involve a two dimensional dynamic Jahn-Teller effect; but only in the latter complex does this correspond with a pseudo compressed CuN_6 chromophore with a tetragonality greater than one, namely, 1.098. In $Cu(tach)_2(ClO_4)_2$ (VIII) the CuN_6 chromophore stereochemistry is clearly elongated rhombic octahedral, but it must be undergoing some two dimensional fluxional behaviour at room temperature comparable to the $Cu(dien)_2XY$ system [61] and the copper Tutton salts [39,45] (Table 7). The $\Delta U^{1/2}$(Cu—L) values clearly support the two dimensional fluxional behaviour for the $Cu(OH_2)_6^{2+}$ cation as demonstrated by the low temperature X-ray crystallography of this complex (section C). The $\Delta U^{1/2}$(Cu—O) data [47] for Cu(methoxyacetate)$_2 \cdot 2\ H_2O$ are of some interest in that all three values are

comparable at ca. 0.1 Å and indicative of fluxional behaviour on all three Cu—O bonds, but are not large enough to represent a fully dynamic situation in this low symmetry space group $P2_1/n$ (as suggested [24] for $Cu(tach)_2(NO_3)_2$ (V)) but are nevertheless of sufficient magnitude to produce a significant change in all three Cu—O bond distances of 0.05 Å when the temperature was lowered to 150 K. Finally the usefulness of the $\Delta U^{1/2}$(Cu—N) values is demonstrated for the two independent CuN_6 chromophores of $Cu(HBpz_3)_2$ (XVI) [62]; both involve an elongated rhombic octahedral CuN_6 chromophore for the same $Cu(HBpz_3)_2$ complex, but with significantly different tetragonalities, 0.792 and 0.866 respectively. The former suggests a static elong-

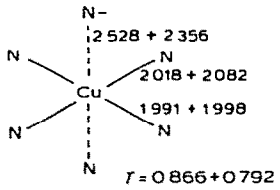

(XVI) $Cu(HBpz_3)_2$-(1)+(2)

ated $Cu(1)N_6$ chromophore with $\Delta U^{1/2}$(Cu—N) values of ca. 0.05 Å (Table 7) while the latter has a significantly higher tetragonality consistent with the presence of some fluxional behaviour which is supported by the $\Delta U^{1/2}$(Cu—N) values (Table 7) indicative of a two dimensional fluxional behaviour consistent with the greater in-plane rhombic distortion of the $Cu(2)N_6$ chromophore in this lattice.

The room temperature data of Tables 6 and 7 not only establish the value of anisotropic temperature factors for indicating the presence of dynamic Jahn-Teller effects in high symmetry crystals, but also for indicating the presence of fluxional behaviour in the stereochemistry of elongated rhombic octahedral CuL_6 chromophores whose differing tetragonalities might otherwise be interpreted as arising from the plasticity effect [4,5] of the copper(II) ion alone.

E. ELECTRON SPIN RESONANCE

This is probably the most important physical technique used in the examination of the electronic properties of fluxional copper(II) systems [2—4,12,20,28]. While the ESR spectra of copper(II) complexes may be measured in the solid state, in solution and (to a lesser extent) in the gaseous state, in order to correlate the observed ESR spectra with the X-ray crystallographic data, the present article restricts the discussion to data obtained in the solid state, either on polycrystalline samples or, preferably, on single-crystals [2,3]. The ESR spectra may be measured using pure copper(II) complexes or as the copper(II) complex diluted in the corresponding zinc(II) complex, as a diamagnetic host lattice. The advantage [2,3] of using concentrated copper(II) complexes is that the ESR data may be directly correlated with the crystallo-

graphic data, but the ESR data are generally limited to the *g*-factors and their directions, as exchange coupling [63] broadens the ESR spectra and masks the hyperfine data. An even more serious disadvantage of measuring the ESR spectra of concentrated copper(II) complexes (as polycrystalline or single-crystal spectra) is that the spectra only yield crystal *g*-factors and only in the case where the local molecular axes of the CuL_6 chromophores of the unit cell (related by the space group elements of symmetry) are aligned parallel i.e. ferrodistortive ordering [38] Fig. 5(a), are the crystal *g*-factors equivalent to the local molecular *g*-factors. In those complexes, where the local molecular axes are misaligned (2γ) by the space group elements of symmetry, Fig. 5(b), (for which antiferrodistortive ordering [5] is the special case, where $2\gamma = 90°$) then resolution of the crystal *g*-factors into their local molecular *g*-factors is necessary, with an uncertainty associated with the precise directions of the local molecular axes in the CuL_6 chromophore, a problem that is most serious in low symmetry stereochemistries [64]. The advantage of measuring the ESR spectrum of a copper(II) complex diluted in a diamagnetic host lattice, i.e. the corresponding zinc(II) complex, is that accurate *g*-factors, copper hyperfine and nitrogen superhyperfine data, along with the *g*-factor directions of the magnetically different, but structurally equivalent misaligned chromophores, are obtained [65]. Although these can be related to the bonding direction of the host lattice they cannot be accurately related to the bonding directions of the doped CuL_6 chromophore, as this is of unknown structure and orientation, and rarely corresponds exactly to the structure of the ZnL_6 chromophore of the host lattice [65,66], even when the pure zinc and copper complexes are nearly isomorphous [67]. The most serious limitation of ESR spectra from a structural point of view is that, although the observed *g*-factors can be shown to be consistent with a stereochemistry (as determined by X-ray crystallography in the solid state), there is no way at present that an ESR spectrum may be used to determine the structure of a copper(II) complex i.e. its Cu—ligand distances and ligand—Cu—ligand bond angles. For this reason although the temperature variation of the ESR spectra of copper(II) complexes have been used to suggest the presence of fluxional behaviour, the low temperature structural data of section C are the major factual basis for the theoretical model for the fluxional systems described in section B, and ESR data only provide supporting evidence. Nevertheless, the temperature variability of the ESR spectra of fluxional copper(II) complexes identified a problem that has only been recently characterised by the use of low temperature X-ray crystallography.

(i) Predicted ESR spectra

Using the model described in Fig. 3(a), (b) and (c), Table 8 lists the predicted ESR behaviour for concentrated copper(II) complexes and copper(II) doped zinc(II) complexes, including the type (i) and (ii) subdivisions, and for the effect of exchange coupling on aligned (AL) and misaligned (ML)

TABLE 8

The predicted behaviour of the ESR spectra of concentrated and dilute fluxional copper(II) complexes, Type A—C, with decreasing temperature [a]

		Concentrated copper(II) systems				Effect of Temp. [b]	Phase Change	Copper(II) doped zinc(II) system		
		Crystal type	Alignment [a]	ESR spectra					No. of equi. sites	Effect of temp.
Type A(i)		Cubic				(a) Isotropic	Yes			(a) No ch.
		or Trigonal	ML	isotropic $g \approx 2.1$—2.15	Dynamic J.T.	(b) Axial	Yes	$g_{iso} + A_{iso}$	1	(b) Axial
						(c) Rhombic	Yes			(c) Rhombic
Type A(ii)		Cubic or Trigonal	ML	isotropic $g \approx 2.1$—2.15	Exchange coupling	(a) Isotropic	No, or Yes?	$g_{iso} + A_{iso}$	3	(a) No ch.
Type B(i)	(a)	Tetragonal or	AL	Axial $g_3 \approx g_2 > g_1 > 2.0$	Pseudo D.J.T.	(a) No ch.	No	$g_3 \approx g_2 > g_1 > 2.0$	1	(a) No ch.
										(b) $g_3 > g_2 \approx g_1 > 2.0$
	(b)	Orthorhombic	ML	Isotropic	Exchange coupling	(b) No ch.	No	$g_3 \approx g_2 > g_1 > 2.0$	2	No ch.
Type B(ii)	(a)	Tetragonal or	AL	Isotropic	Exchange coupling	(a) No ch.	No	$g_3 > g_2 \approx g_1 > 2.0$	2	No
	(b)	Orthorhombic	ML	Isotropic	Exchange coupling	(b) No ch.	No	$g_3 > g_2 \approx g_1 > 2.0$	4	No

TABLE 8 (Continued)

		Concentrated copper(II) systems				Effect of Temp. [b]	Phase Change	Copper(II) doped zinc(II) system		
		Crystal type	Alignment [a]	ESR' spectra					No of equi. sites	Effect of temp.
Type C(i)	(a)	Monoclinic	AL	$g_3 > g_2 > g_1 > 2.0$	≈static	Changes to more axial	No	$g_3 > g_2 > g_1 > 2.0$	1	Change to more axial
		or								
	(b)	Triclinic	ML	Isotropic	Exchange coupling	No ch.	No	$g_3 > g_2 > g_1 > 2.0$	2	Change to more axial
Type C(ii)	(a)	Monoclinic	AL	$g_3 > g_2 \approx g_1 > 2.0$	Static	No ch.	No	$g_3 > g_2 > g_1 > 2.0$	1	No
		or								
	(b)	Triclinic	ML	Isotropic	Exchange coupling		No	$g_3 > g_2 > g_1 > 2.0$		No

[a] Abbreviations: AL = CuL_6 chromophores aligned; ML = misaligned; No ch. = no change.

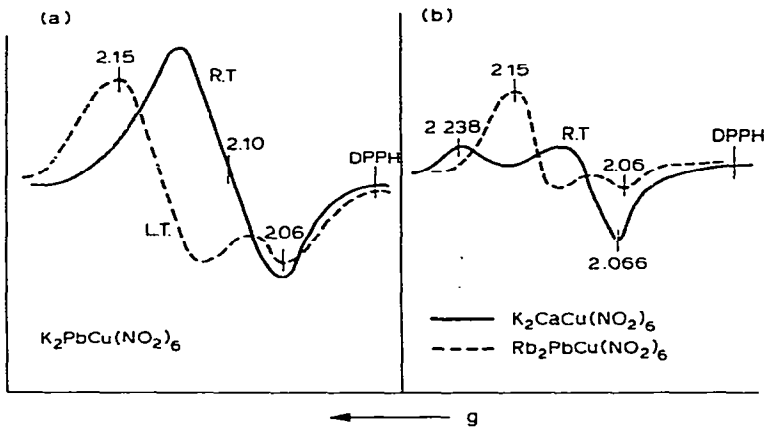

Fig. 7. The powder ESR spectra of some $M^{I}M^{II}Cu(NO_2)_6$ complexes.

local molecular axes. The following text describes the observed behaviour in each class separately and gives some typical examples.

Type A(i) concentrated

Historically the first system to be observed with an isotropic ESR spectrum * [23,28,68—70] was the cubic $K_2PbCu(NO_2)_6$ complex, $g_i = 2.10$ (Table 9), arising from the dynamic Jahn-Teller effect and involving three potential wells of equal energy, which are thermally accessible, $B < kT$, Fig. 7(a). More recently [21] $Tl_2PbCu(NO_2)_6$, has been shown to have an isotropic ESR spectrum $g_i = 2.124$. A regular tris(chelate)copper(II) complex [2,3,71] has D_3 symmetry and generates a ^2E ground state, for the d^9 configuration of the copper(II) ion, which is also Jahn-Teller unstable, and produces an isotropic ESR spectrum, as in $Cu(en)_3(SO_4)$ [72—78], Fig. 8(a), and $Cu(ompha)_3(ClO_4)_2$ [44] complexes, which both crystallise in a high symmetry space group [27,44]. The CuO_6 chromophore in the trigonal crystals [79—81] of $Cu(PyNO)_6X_2$ where $X = NO_3^-$ or ClO_4^- yields isotropic ESR spectra [82,83] in the concentrated complex, $g_i = 2.19$.

Type A(i) Dilute

The ESR spectra of copper(II) doped systems of high symmetry are remarkably limited; the only dilute hexanitro system known is $Cu/Cs_2SrCd(NO_2)_6$

* Caution: the observation of an isotropic ESR spectrum [2,3] for a concentrated copper(II) complex is only diagnostic of a dynamic Jahn-Teller system if, (a) six equivalent ligands are present, and (b) the crystal system is of high symmetry i.e. cubic or trigonal. An isotropic ESR spectrum can also be observed when misalignment of the local molecular axes is present (Fig. 5) and exchange coupling [63] results in an isotropic signal.

TABLE 9

Type A ESR spectra for concentrated copper(II) complexes and copper(II) doped complexes

Complex	Stereochemistry	Crystal	Temp.	g-factor
Type A(i) concentrated				
$K_2PbCu(NO_2)_6$	Octahedral	Cubic	R.T.	2.10
$Tl_2PbCu(NO_2)_6$	Octahedral	Cubic	R.T.	2.124
$Cu(en)_3(SO_4)$	Trigonal	Hexagonal	R.T.	2.13
$Cu(ompha)_3(ClO_4)_2$	Trigonal	Hexagonal	R.T.	2.25
$Cu(PyNO)_6(ClO_4)_2$	Trigonal	Trigonal	R.T.	2.19
$Cu(PyNO)_6(NO_3)_2$	Trigonal	Trigonal	R.T.	2.19
Type A(i) dilute				
$Cu/Cs_2SrCd(NO_2)_6$	Octahedral	Cubic	R.T.	
$Cu/Zn(en)_3(NO_3)_2$	Trigonal	Hexagonal	R.T.	2.139
$Cu/Zn(bipy)_3(NO_3)_2 \cdot 5\ H_2O$	Trigonal	Hexagonal	R.T.	2.116
$Cu/Zn(bipy)_3SO_4 \cdot 7\ H_2O$	Trigonal	Monoclinic	R.T.	2.10
$Cu/Zn(hfacac)_3[C_{14}H_{19}N_2]$	Trigonal	Monoclinic	R.T.	2.11
$Cu/Zn(phen)_3(NO_3)_2 \cdot 2\ H_2O$	Trigonal	Triclinic	R.T.	2.12
Type A(ii) concentrated, Type A(ii) dilute				
No known examples				

[84], which is reported to have an isotropic ESR spectrum at room temperature. Isotropic ESR spectra are also reported for the hexagonal system copper doped $Zn(en)_3(NO_3)_2$ [74,85] and $Zn(bipy)_3(NO_3)_2 \cdot 5\ H_2O$ [85] and also in the lower symmetry systems of copper doped $Zn(bipy)_3SO_4 \cdot 7\ H_2O$ [76], $Zn(hfacac)_3[C_{14}H_{19}N_2]$ [86] and $Zn(phen)_3(NO_3)_2 \cdot 2\ H_2O$ [57], the first two of which are monoclinic and the last triclinic. In these lower symmetry systems a near octahedral CuN_6 or CuO_6 chromophore must be present with three near equivalent potential wells (Fig. 3(a)).

Type A(ii)

There have been no examples of either concentrated or dilute copper(II) complexes exhibiting Type A(ii) behaviour.

Type B(i) concentrated

The ESR spectrum for the situation of Fig. 3(b)(i), with two equivalent low energy wells is predicted [28,87,88] to be axial, but pseudo compressed in type, i.e. $g_\perp > g_\parallel > 2.0$ and not that associated with a genuine compressed type ESR spectrum [2,3], namely, $g_\perp > g_\parallel \approx 2.0$. The pseudo compressed type ESR spectrum [30,89] is observed for complexes with a pseudo compressed geometry, such as $Rb_2PbCu(NO_2)_6$ [29] Fig. 7(b), and $Cs_2PbCu(NO_2)_6$ (I) [30] where the orthorhombic space group is such that the local molecular axes are aligned parallel (Table 10(a)), the ESR spectrum is axial with the

TABLE 10

Type B ESR spectra for concentrated copper(II) complexes and copper(II) doped complexes, with aligned (AL) and misaligned (ML) local molecular axes (P.C.O. = pseudo compressed octahedral; E.T.O. = elongated tetragonal octahedral)

Complex	Stereochemistry	Crystal	Temp.	g_1	g_2	g_3
Type B(i) concentrated						
$Rb_2PbCu(NO_2)_6$	P.C.O.	Orthorhombic (AL)	R.T.	2.064		2.150
$Cs_2PbCu(NO_2)_6$ (I)	P.C.O.	Orthorhombic (AL)	R.T.	2.066		2.156
$Cu(dien)_2(NO_3)_2$ (II)	P.C.O.	Orthorhombic (ML)	R.T.		2.102 (see text)	
$Cu(C_5H_5NO)_6(ClO_4)_2$		Hexagonal (ML)	L.T.	2.08	2.22	2.24
$Cu(C_5H_5NO)_6(NO_3)_2$		Hexagonal (ML)	L.T.	2.075	2.221	2.238
$Cu(tach)_2(NO_3)_2$	Near octahedral	Monoclinic (AL)	R.T.		2.13	
			ca. 120 K	2.068	2.154	2.171
			>40 K	2.047	2.081	2.250
$K_2PbCu(NO_2)_6$ (III)	P.C.O.	Orthorhombic (ML)	195 K	2.06		2.15
$Cu(en)_3(SO_4)$ (IV)	P.C.O.	Triclinic	120 K	2.06		2.16
K_2CuF_4 (XIV)	Antiferrodistortive	Tetragonal (ML)	R.T.	2.09		2.28
Ba_2CuF_6 (XV)	Antiferrodistortive	Tetragonal (ML)	R.T.	2.05	2.20	2.36
Type B(i) dilute						
$Cu/Zn(dien)_2(NO_3)_2$ (XVII)	P.C.O.	Orthorhombic (ML)	R.T.	2.05	2.147(90)	2.16(102)
$Cu/Zn(dien)_2(ClO_4)_2$	P.C.O.	Cubic (ML)	R.T.	2.063		2.166(86)
Type B(ii) dilute						
$Cu/Zn(phen)_3(NO_3)_2 \cdot 2\,H_2O$	E.T.O.	Triclinic (AL)		2.064	2.085	2.273

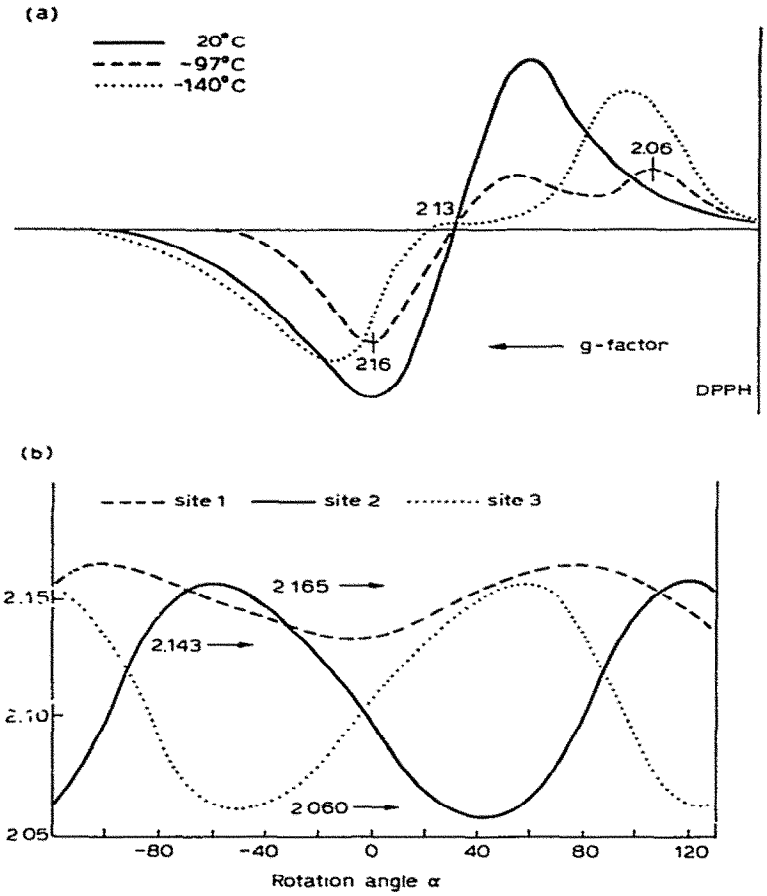

Fig. 8. (a) The powder ESR spectrum of $Cu(en)_3SO_4$. (b) The single crystal ESR spectrum of $Cu(en)_3SO_4$ rotation about the axis at 55° to the C_3 axis (140 K).

lowest g-value, $g_{\parallel}$, clearly above 2.0 and not approximately equal to 2.0, as required for a genuine compressed octahedral stereochemistry [2,3]. The effect of temperature on the isotropic ESR spectra of $K_2PbCu(NO_2)_6$ (III) [23,28,68—70] and $Cu(en)_3(SO_4)$ (IV) [72—78] both show a characteristic change to an axial spectrum, Figs. 7(a) and 8(a) respectively, with $g_{\parallel} < g_{\perp}$, but significantly greater than 2.0, again characteristic of a pseudo compressed ESR spectrum and consistent with the observed pseudo compressed stereochemistries (IIIL and IVL, respectively) observed at low temperature. The single-crystal ESR spectrum [72—78] of $Cu(en)_3(SO_4)$ (IV) at low temperature, Fig. 8(b), reveals three equivalent magnetic sites, with the g-values 2.060, 2.143 and 2.165 in the triclinic space group of the low temperature structure, consistent with the presence of three separate mosaic phases. Cu-

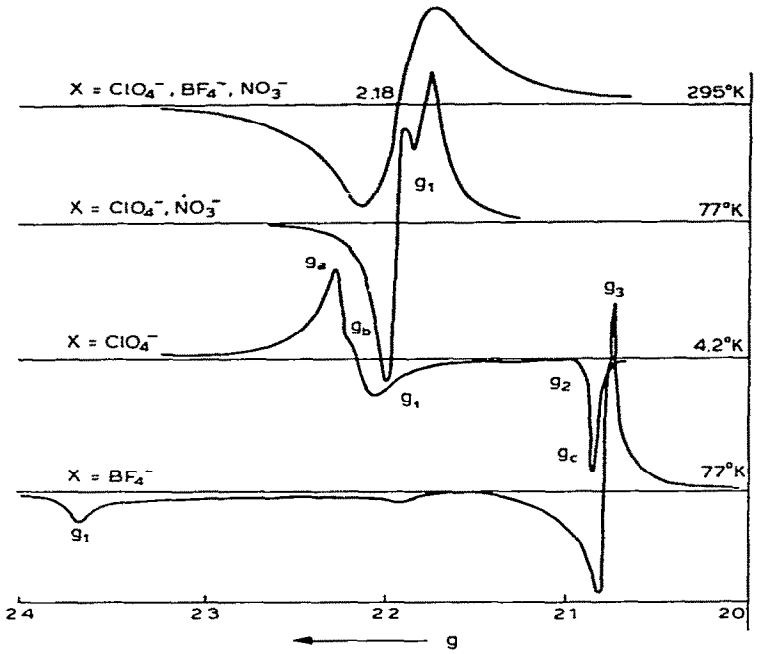

Fig. 9. The powder ESR spectra of some $Cu(PyNO)_6X_2$ complexes, where X = BF_4^-, NO_3^- and ClO_4^-, at 295 and 77 K. Reproduced by permission of the authors [83].

$(dien)_2(NO_3)_2$ (II) crystallises in the orthorhombic space $P2_12_12_1$ [31] and gives [90] an isotropic signal, 2.102 in a powder sample, which only yields very slight anisotropy in the single crystal g-factors of $g_a = 2.1034$, $g_b = 2.1179$ and $g_c = 2.1350$, due to almost complete misalignment of the four CuN_6 chromophores in the unit cell ($2\gamma = 80°C$). An attempt to resolve [84] the crystal g's into their local molecular g-factors, although subject to some uncertainty, yielded the g-factors 2.052, 2.144 and 2.159 (pseudo reversed), which are consistent with a pseudo compressed rhombic octahedral stereochemistry for the local CuN_6 chromophore consistent with the room temperature crystal structure (IIR), with the lowest g-factor, 2.052, correlating with the short N—CU—N direction. The single-crystal ESR spectra showed only a slight variation with temperature, consistent with the lack of variation of either the space group or the CuN_6 stereochemistry with decreasing temperature (IIL).

$Cu(pyNO)_6X_2$, where X = ClO_4^- and BF_4^-, crystallise [79—82] in the trigonal space group $R\bar{3}$ with six equivalent Cu—O distances, 2.08—2.09 Å, the powder ESR spectra [82] are isotropic at room temperature, Fig. 9, but at 100 K are slightly anisotropic in the trigonal space group (2.168/2.190 and 2.174/2.179, respectively). At 4.2 K both spectra are anisotropic, but quite different; the perchlorate involves a normal elongated type of spectrum with $g_a = 2.375$, $g_b = 2.079$, and $g_c = 2.075$ while the tetrafluoroborate has a pseudo compressed type spectrum, $g_a = 2.235$, $g_b = 2.225$ and $g_c = 2.083$,

consistent [83] with a ferrodistortive and antiferrodistortive order [82], respectively, in this pair of cation distortion isomers. The ESR spectrum [24] of $Cu(tach)_2(NO_3)_2$ (V) is isotropic at room temperature, consistent with the near regular octahedral CuN_6 stereochemistry at room temperature, $T = 0.99$, in this monoclinic space group $C2/m$ [24]. The local molecular axes of the CuN_6 chromophores are aligned; hence the isotropic ESR arises from the near electronically degenerate ground state and a near equivalent three potential well system (Fig. 3(a)). The spectrum becomes anisotropic at low temperature and above 120 K, pseudo compressed in form, consistent with the pseudo compressed octahedral stereochemistry [36] of the structure at 120 K (VL). The ESR spectrum at 4 K (2.047, 2.081 and 2.250) is consistent with an axial elongated CuN_6 stereochemistry, as observed [24] in $Cu(tach)_2(ClO_4)_2$ (VIII) and suggests that the CuN_6 chromophore of $Cu(tach)_2(NO_3)_2$ may undergo a near dynamic Jahn-Teller behaviour at room temperature, a pseudo dynamic Jahn-Teller behaviour at ca. 120 K and a purely static behaviour at 4.2 K. Thus the variation of the ESR spectrum of $Cu(tach)_2(NO_3)_2$ with decreasing temperature, illustrates the three types of behaviour predicted in Fig. 3(a–c), although the final confirmation must await a low temperature crystal structure determination below 93 K to confirm the static elongated rhombic octahedral stereochemistry of the CuN_6 chromophore.

The powder ESR spectra [13,84] of K_2CuF_4 (XIV) and Ba_2CuF_6 (XV) are axial ($g_\parallel = 2.09$ and $g_\perp = 2.28$) and rhombic ($g_1 = 2.05$, $g_2 = 2.20$ and $g_3 = 2.36$), respectively, consistent with earlier X-ray structure determinations [33,34] involving aligned compressed axial and rhombic compressed CuF_6 octahedra. But in view of the pseudo compressed type ESR spectra the structures have been re-examined and shown [59,60] to be consistent with antiferrodistortive ordering in the plane at right angles to the c-axes, consequently the crystal g-factors in this plane are not equivalent to the local molecular g-factors and must be resolved into their local molecular g-factors, complicated in the case of the Ba_2CuF_6 (XV) complex by the presence of non-linear Cu—F—Cu bridging angles [34].

Type B(i) dilute

The ESR spectra of the copper(II) doped $Zn(dien)_2(NO_3)_2$ (orthorhombic) (XVI) [32,65,91] and $Zn(dien)_2(ClO_4)_2$ (cubic) [91] are both pseudo compressed in type (Table 10) with the highest A-values (in parentheses) on the

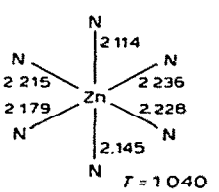

(XVI) $Zn(dien)_2(NO_3)_2$(orthorhombic)

highest g-values; spectra that are consistent with the compressed rhombic

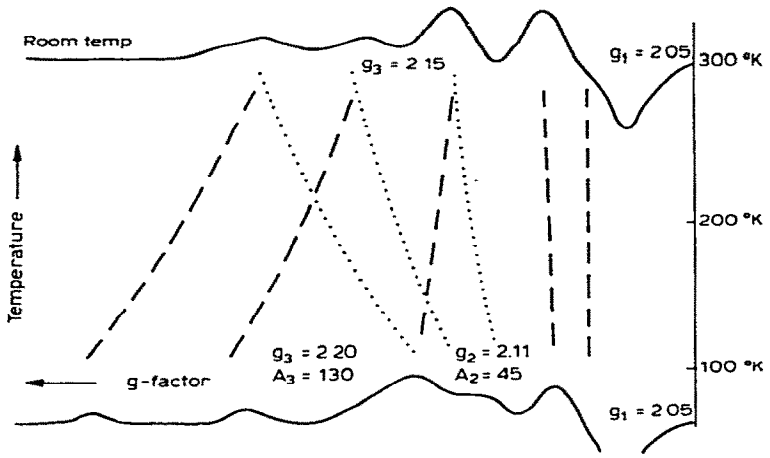

Fig. 10. Temperature variation of g-factors for copper doped Cu/Zn(dien)$_2$(NO$_3$)$_2$.

octahedral geometry of Cu(dien)$_2$(NO$_3$)$_2$ (II) [31] and Zn(dien)$_2$(NO$_3$)$_2$ (XVII) [91]. But unlike the lack of temperature effect on either the compressed tetragonal octahedral CuN$_6$ chromophore of Cu(dien)$_2$(NO$_3$)$_2$ (II) or its isotropic ESR spectrum the copper(II) doped Zn(dien)$_2$(NO$_3$)$_2$ (XVI) ESR spectrum changes dramatically with decreasing temperature (Fig. 10) from a pseudo compressed to an elongated tetragonal octahedral type. The behaviour is consistent with a pseudo dynamic Jahn-Teller effect in the copper doped Zn(dien)$_2$(NO$_3$)$_2$ (XVI) at room temperature, (Fig. 3(b)) with almost equal thermal occupation of Wells II and III, which at low tempera-

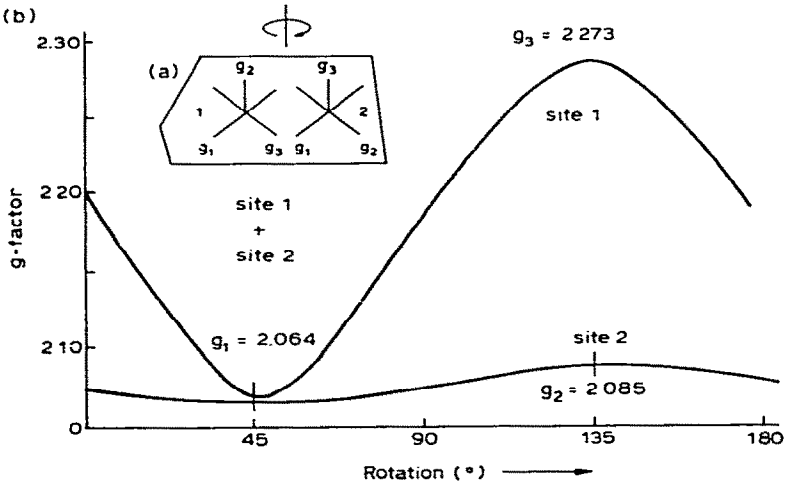

Fig. 11. Copper doped Zn(phen)$_3$(NO$_3$)$_2$ · 2 H$_2$O (a) crystal morphology and g-factors for sites 1 and 2; (b) single crystal rotation spectra about g_2 of site 1 and g_3 of site 2.

ture changes to a single dominant low energy potential Well II (Fig. 3(c)) and having the ESR spectrum consistent with an elongated tetragonal octahedral CuN_6 chromophore.

Type B(ii) concentrated or dilute

No examples are known for a copper(II) complex in which there is ESR evidence for two thermally isolated and 90° misaligned CuL_6 chromophores, but there is evidence for their existence in the low temperature (91 K) single crystal ESR spectrum [57] of copper(II) doped $Zn(phen)_3(NO_3)_2 \cdot 2\ H_2O$ (Fig. 11). As the complex crystallises in the triclinic space group $P\bar{1}$, the local molecular axes of the ZnN_6 chromophores are aligned parallel, so the two 90° misaligned sites must be at crystallographically equivalent centres and hence fulfil the conditions for two equal potential wells, thermally isolated by a potential barrier $B > kT$, Fig. 3(B)(ii).

Type C(i) concentrated

The ESR spectrum predicted for the situation of Fig. 3(c)(i) is $2.0 < g_1 \approx g_2 < g_3$ with $R = g_2 - g_1/g_3 - g_2$, clearly less than 1.0, a spectrum that is consistent with an elongated tetragonal octahedral structure, [2,3] but if $B < RT$ the g-factors will be temperature variable. In high symmetry systems the temperature variability is marked, as in $Cu(ompha)_3(ClO_4)_2$ (VII), Fig. 12, where an isotropic g-factor of 2.25 [44] is obtained in the hexagonal room temperature lattice, which at low temperature becomes triclinic, yielding rhombic, 2.06, 2.12 and 2.52 g-factors (with copper hyperfine on the highest g-factor) with $R = 0.15$, consistent with an elongated tetragonal octahedral CuO_6 chromophore in the lower symmetry triclinic space group. Comparable changes occur in the ESR spectrum [85] of $Cu(bipy)_3(NO_3)_2 \cdot 5\ H_2O$ (Table 11) which although of unknown structure crystallises [85] in the hexagonal

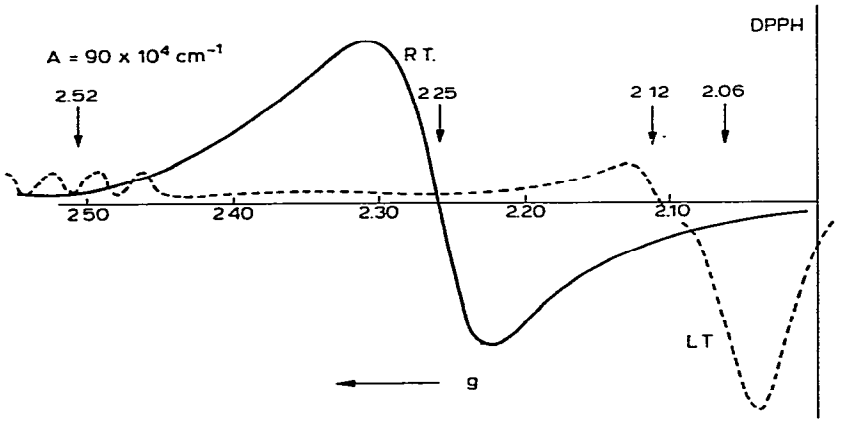

Fig. 12. The powder ESR spectrum of $Cu(ompha)_3(ClO_4)_2$. Reproduced by permission of the authors [44].

TABLE 11

Type C g-factors, R-values [a] and tetragonalities of some orthorhombic, monoclinic and triclinic concentrated complexes and their temperature variation

Complex	Room temperature						Low temperature				
	Sp. Gr.	g_1	g_2	g_3	R	T_{RT}	g_1	g_2	g_3	R	T_{LT}
Type C(i) concentrated											
$Cu(bipy)_3(NO_3)_2 \cdot 5\ H_2O$			2.119				2.082		2.250 [c]		
$Cu(bipy)_3SO_4 \cdot 7\ H_2O$	C_2/c		2.107			0.95	2.075		2.25		
$(NH_4)_2Cu(OH_2)_6(SO_4)_2$	$P2_1/a$	2.071	2.218	2.360	0.97	0.914	2.076	2.131	2.433	0.18	0.865
$Cu(dien)_2Br_2 \cdot H_2O$	$P2_1/c$	2.043	2.097	2.213	0.47	0.86	2.043	2.065	2.230	0.13	
$Cu(dien)_2Cl_2 \cdot H_2O$	$P2_1/c$	2.050	2.070	2.210	0.14	0.85	2.049	2.090	2.226	0.30	
$Cu(terpy)_2(NO_3)_2$	$14_1/a$	2.038	2.103	2.255	0.43	0.89	2.044	2.083	2.263	0.22	
$Cu(methoxyacetate)_2 \cdot 2\ H_2O$	$P2_1/n$	2.087	2.185	2.360	0.54	1.115	2.069	2.118	2.441	0.22	1.084
$Cu(tach)_2(NO_3)_2$	$C2/m$	2.113 [b]	2.138 [b]	2.145 [b]	3.57 [b]	0.99	2.047	2.081	2.250	0.20	1.073
$Cu(tach)_2(ClO_4)_2$	$Cmca$	2.086 [b]	2.106 [b]	2.190 [b]	0.24 [b]	0.88	2.061	2.100	2.203	0.38	
Type C(ii) concentrated Normal static systems											

[a] $R = g_2 - g_1/g_3 - g_2$ for $g_3 > g_2 > g_1$. [b] Based on crystal g-values. [c] Copper hyperfine $A_3 = 153 \times 10^3\ cm^{-1}$.

TABLE 12

Bond length data and tetragonality, for some tetragonal octahedral CuL_6 and ZnL_6 chromophores, using the atom numbering of $Cu(ompha)_2(ClO_4)_2$ (VII)

Complex	Cu–X_1	Cu–X_2	Cu–X_3	Cu–X_4	Cu–X_5	Cu–X_6	Tetragonality
$Cs_2PbCu(NO_2)_6$	2.232	2.227	2.227	2.232	2.070	2.070	1.077
$Cu(bipy)_3(ClO_4)_2$	2.035	2.034	2.026	2.030	2.450	2.226	0.87
$Cu(bipy)_3(SO_4) \cdot 7\ H_2O$	2.07	2.06	1.98	2.10	2.21	2.26	0.95
$Cu(dien)_2Br_2 \cdot H_2O$	2.04	2.07	2.03	2.13	2.46	2.35	0.86
$Cu(dien)_2Cl_2 \cdot H_2O$	2.036	2.118	2.034	2.073	2.372	2.466	0.853
$Cu(dien)_2Cl(ClO_4)$	2.037	2.089	2.025	2.036	2.386	2.516	0.835
$Cu(terpy)_2(NO_3)_2$	2.012	2.085	1.960	2.012	2.288	2.288	0.890
$Cu(hfacac)_2py_2$	2.021–N	2.003–N	2.002–O	1.994–O	2.266–O	2.300–O	0.878
$Cu(C_5H_4NSO_3)_2 \cdot 2\ H_2O$	1.976–O	2.034–N	1.976–O	2.034–N	2.344–O	2.344–O	0.88
β-$Cu(NH_3)_2Br_2$	2.87–Br	2.87–Br	2.87–Br	2.87–Br	2.03–N	2.03–N	1.41
$Cu(NH_3)_2(C_2O_4) \cdot 2\ H_2O$	2.15–O	2.10–O	2.15–O	2.10–O	1.98–N	1.98–N	1.07
$Cu(fomp)_2(meen)$	2.240–N	2.240–N	2.317–O	2.317–O	1.901–O	1.901–N	1.20
	Zn–X_1	Zn–X_2	Zn–X_3	Zn–X_4	Zn–X_5	Zn–X_6	
$Zn(hfacac)_2py_2$	2.12–N	2.12–N	2.16–O	2.16–O	2.07–O	2.07–O	1.034
$Zn(dien)_2Br_2 \cdot H_2O$	2.22	2.24	2.28	2.27	2.18	2.13	1.045
$Zn(C_5H_4NSO_3)_2 \cdot 4\ H_2O$	2.14–O	2.13–O	2.14–O	2.13–O	2.09–N	2.09–N	1.022

space group *P6cc*, to give low temperature *g*-factors (Table 11) which are comparable to those for $Cu(bipy)_3(ClO_4)_2$ [92] which has a static elongated tetragonal stereochemistry ($T = 0.87$), Table 12. A potentially less complicated system is that of $Cu(phen)_3(NO_3)_2 \cdot 2\ H_2O$ (XIII) [57,93] which crystallises in the triclinic space group $P\bar{1}$ with only two molecules in the unit cell with a relatively high tetragonality [57] of 0.95 and yields an isotropic powder ESR spectrum [92] of 2.134, but with a spread of *g*-values (2.110, 2.187, 2.2025) in the single-crystal rotation spectrum. The powder ESR spectrum becomes axial at liquid nitrogen temperature including copper hyperfine structure with $g_{\parallel} = 2.273$ ($A_{\parallel} = 161 \times 10^{-4}$ cm^{-1}) and $g_{\perp} = 2.062$ ($A_{\perp} = 36 \times 10^{-4}$ cm^{-1}) which are consistent with a clear axially elongated stereochemistry (XIIIL), observed at 153 K and the ESR spectrum does not change down to liquid helium temperature [92]. Full single-crystal rotation data [57] (involving copper hyperfine splitting) confirms the clear increase in anisotropy of the *g*-factors with decreasing temperature, with the *g*'s lying along the Cu—N bond directions and predicting an elongated rhombic octahedral stereochemistry for the CuN_6 chromophore at liquid nitrogen temperature, (XIIIL) with evidence for only one magnetic site, a behaviour that contrasts with that observed [57] in the copper doped $Zn(phen)_3(NO_3)_2 \cdot 2\ H_2O$ system where two distinct magnetic sites were observed (Table 9). $Cu(bipy)_3SO_4 \cdot 7\ H_2O$ crystallises [76] in the monoclinic space group $C2/c$ with a high tetragonality of 0.95 (Table 12) and has an isotropic *g*-factor at room temperature, possibly due to misalignment, but resolves out into an axial ESR spectrum at low temperature (Table 11) consistent with an elongated tetragonal octahedral CuN_6 chromophore stereochemistry.

In the monoclinic system of $(NH_4)_2Cu(OH_2)_6(SO_4)_2$ (VI) [51,52] although complicated by misalignment of the CuO_6 chromophores ($2\gamma = 80°$), the absence of exchange coupling allows the direct observation of the local molecular *g*-factors [94,95]. At room temperature the *g*-factors are clearly rhombic (Table 11) with $R \approx 1.0$ suggesting a stereochemistry intermediate

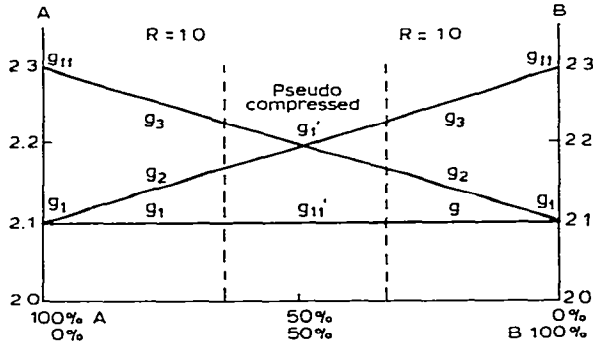

Fig. 13. The effect of mixing two CuN_6 chromophores A and B misaligned by 90° as a function of the % composition ($R = g_2 - g_1/g_3 - g_2$ with $g_3 > g_2 > g_1$).

between elongated rhombic and compressed rhombic octahedral, an interpretation that is clearly at variance with the room temperature structure of this complex (VIR) [51,52]. The g-factors change significantly at low temperature [94,95] in a quite characteristic way; the lowest g-factor remains temperature invariant, the intermediate g-factor decreases with decreasing temperature and the highest g-factor shows a most significant increase in value (Table 11). The net result is a significant increase in the R-value to 5.49, well above 1.0 and consistent with an elongated rhombic octahedral stereochemistry of the CuO_6 chromophore. In the case of $(NH_4)_2Cu(OH_2)_6(SO_4)_2$ (VI) these changes parallel the decrease in tetragonality [39] of the CuO_6 chromophore from 0.914 to 0.865 described in section C, and may be understood in terms of the potential energy system, described in Fig. 3(c)(i) in which one elongated rhombic octahedral well (Well II) dominates, but there is a significant contribution of Well III through thermal mixing, with B clearly less than kT. The way in which the apparent g-factors vary with the percentage composition of the potential Wells II and III of Fig. 3(c)(i) is illustrated in Fig. 13. For two elongated tetragonal chromophores A and B with equivalent g-factors, $g_\parallel$ and $g_\perp$, an equal mixture of A and B with their tetragonal axes misaligned by 90°, the situation of Fig. 3(b)(i) and illustrated in Fig. 4, would correspond to $g_\perp' = (g_\perp + g_\parallel)/2$ and $g_\parallel' = g_\perp$ giving $g_\perp' > g_\parallel' > 2.0$, which is the correct sense for a pseudo reversed type of ESR spectrum and corresponds to a pseudo compressed tetragonal octahedral stereochemistry. The significance of Fig. 13 is that even the presence of 36% of either A or B radically changes the appearance of the ESR spectrum from axially elongated ($g_\parallel > g_\perp > 2.0$) to an intermediate form with $g_3 > g_2 > g_1 > 2.0$ and $R \approx 1.0$ as in the case of $(NH_4)_2Cu(OH_2)_6(SO_4)_2$ (VI) for which $R = 0.97$, suggesting that there is a 64/36% mixture of the elongated stereochemistries in the ground state of the fluxional ammonium Tutton salt at room temperature. A number of complexes clearly exhibit less than 36% fluxional character [95], thus the three complexes $Cu(dien)_2Cl_2 \cdot H_2O$ [61], $Cu(dien)_2Br_2 \cdot H_2O$ [96] and $Cu(terpy)_2(NO_3)_2$ [97], Table 12, all involve elongated rhombic octahedral stereochemistries and yield rhombic g-factors (Table 11) [61,98] with R values < 1.0, but their g-factors are still temperature variable (Table 11) but with much smaller, low-temperature, R-values. Such complexes are only slightly fluxional and correspond with the potential energy diagram of Fig. 3(c)(i). The varying tetragonality of the Tutton salts of Fig. 6 reflects the differing degrees of fluxional behaviour [39] of the $Cu(OH_2)_6^{2+}$ cations present, which is reflected in the non-temperature variability of the g-factors [99] of the caesium salt and only slight temperature variability of the rubidium salt.

The g-factors of Cu(methoxyacetate)$_2 \cdot 2\ H_2O$ (IX) [100] are clearly rhombic with $R = 0.54$ (Table 11) and follow the same characteristic variation with temperature as observed for the Tutton salt [94], but with one slight difference, namely, the lowest g-factor also decreases slightly with temperature. This implies that although the fluxional involvement of Wells II and III is the dominant factor (Fig. 3(c)(i)) the potential barrier between Wells I

TABLE 13

Type C g- and A-factors ($\times 10^{-4}$ cm^{-1}) for fluxional copper(II) doped zinc(II) systems at room temperature and at the temperature of liquid nitrogen, ca. 77 K

Host Lattice	Room temperature (ca. 295 K)						
	g_1	A_1	g_2	A_2	g_3	A_3	R
Type C(i) dilute							
$Zn(en)_3(NO_3)_2$			2.139	56			
$Zn(bipy)_3(NO_3)_2 \cdot 5\ H_2O$			2.116				
$Zn(bipy)_3(SO_4)_2 \cdot 7\ H_2O$			2.138				
$Zn(C_5H_5NO)_6(ClO_4)_2$	2.030	9			2.367	103	
Zn(tetramethylene sulphoxide)$_6$(ClO_4)$_2$	2.075				2.38	133	
Zn(N-methylimidazole)$_6$(ClO_4)$_2$	2.061	13			2.277	171	
$Zn(imidazole)_6Cl_2 \cdot 4\ H_2O$			2.170	57.7			
$Ba_2Zn(HCO_2)_6 \cdot 4\ H_2O$	2.11	34			2.340	98	
$K_2Zn(OH_2)_6(SO_4)_2$	2.033	58	2.0252	52	2.322	57	(191 K)
$Mg(OH_2)_6H_2edta$	2.033	61	2.198	27	2.355	95	
$Zn(hfacac)_2py_2$	2.113	9	2.116	23	2.278	104	
Site 1							
Sites 2 and 3							
$Zn(dien)_2Br_2 \cdot H_2O$	2.033	<25	2.113	51	2.204	127.3	
$Zn(C_5H_4NSO_3)_2 \cdot 4\ H_2O$	2.030	74	2.202	56	2.263	53	2.82
	2.055	77	2.221	42	2.284	63	2.64
Zn(methoxyacetate)$_2$ · 2 H_2O	2.077	109			2.328	<25	
$Zn(NH_4)_2(NH_3)_2(CrO_4)_2$	2.017	147	2.216	10	2.230	10	
Type C(ii) dilute							
Zn(pyrazine)(SO_4) · 3 H_2O	2.109	64	2.214	25	2.412	119	

and II is low enough in Cu(methoxyacetate)$_2$ · 2 H_2O for some thermal occupation of Well I to be involved, in other words the room temperature structure must involve thermal mixing of all three elongated chromophores misaligned by 90°, proportional to the thermal occupation of the potential Wells I, II and III.

Thus the best guide to the presence of fluxional behaviour is the room temperature tetragonality (T): if this lies in the range 0.90—0.99 for a six coordinate chromophore then some fluxional effects (or disorder) are the most likely explanation of the observed isotropic or pseudo rhombic g-factors.

Type C(i) dilute

In the trigonal class, the Cu/$Zn(en)_3SO_4$ system [74,85] does not appear to exist, although the corresponding Cu/$Zn(en)_3(NO_3)_2$ system has been reported

Liquid nitrogen temperature (ca. 77 K)						
g_1	A_1	g_2	A_2	g_3	A_3	Temp. (K)
2.082				2.248	168	120
2.077				2.260	157	93
2.068				2.268	150	93
2.080	9			2.367	103	77
2.090	18			2.41	125	77
2.065	13			2.307	165	77
2.088	37.5			2.300	158.3	90
2.08	18			2.390	131	90
2.030	59.6	2.200	36.0	2.364	76.0	77
2.033	60.7	2.150	<20	2.420	96.5	4.2
2.028	77	2.185	41	2.365	105	77
2.073				2.340	144	133
2.070	4	2.089	3.0	2.344	151	4.2
2.074	12.5	2.226	104	2.242	107	4.2
2.033	<25	2.065	<25	2.236	155.3	77
2.055	83	2.1435	25	2.362	100	91
2.078	110			2.329	<25	93
2.014	144.6	2.109	42.9	2.287	26.2	77
2.109		2.214		2.414		77

[74,85] (Table 13) to have an isotropic signal at room temperature, $g_i = 2.139$ and $A_i = 56 \times 10^{-4}$ cm^{-1}, which is slightly anisotropic in the single-crystal data, $g_\parallel = 2.153$ and $A_\parallel = 68 \times 10^{-4}$ cm^{-1}, $g_\perp = 2.129$ and $A_\perp = 50 \times 10^{-4}$ cm^{-1}. Below 70 K the powder spectrum becomes anisotropic characteristic of an elongated tetragonal CuN_6 chromophore, $g_\parallel = 2.248$, $A_\parallel = 168 \times 10^{-4}$ cm^{-1} and $g_\perp = 2.082$, with no hyperfine observed on $g_\perp$. The spectrum of a single crystal at low temperature is highly complex, but may be interpreted using the extreme g-values from the powder spectra to involve six equivalent magnetic sites related by the original six-fold axis of the $P6_322$ space group. From an analysis of the temperature variation of the line width [74], associated with the highest g-factor, the height of the potential energy barrier of $\Delta_{II,III}$ was estimated to be 102 ± 2 cm^{-1} consistent with the value obtained in the $Cu/K_2Zn(OH_2)_6(SO_4)_2$ system of 120 cm^{-1} [101] (see later).

The powder ESR spectrum of 10% $Cu/Zn(bipy)_3(NO_3)_2 \cdot 5\ H_2O$ [85] is isotropic at room temperature ($g_2 = 2.116$, Table 13) with no evidence for copper hyperfine and becomes anisotropic at low temperature, $g_\perp = 2.077$ and $g_\parallel = 2.260$ ($A_\parallel = 157 \times 10^{-4}\ cm^{-1}$) values consistent with an elongated rhombic octahedral CuN_6 chromophore stereochemistry. The single-crystal ESR spectra indicate the presence of six near equivalent magnetic sites, comparable to the situation in the $Cu/Zn(en)_3(NO_3)_2$ system [74, 85].

1% $Cu/Zn(bipy)_3SO_4 \cdot 7\ H_2O$ [76] also yields an isotropic ESR spectrum ($g_2 = 2.138$, Table 13) which becomes anisotropic at liquid nitrogen temperature; $g_\perp = 2.068$ and $g_\parallel = 2.268$ ($A_\parallel = 150 \times 10^{-4}\ cm^{-1}$) clearly indicative of fluxional behaviour, but the single-crystal spectra showed the presence of two magnetically equivalent sites ($2\delta = 130^\circ$), $g_1 = 2.070$, $g_2 = 2.15$ ($A_2 = 70 \times 10^{-4}\ cm^{-1}$) and $g_3 = 2.270$ ($A_3 = 152 \times 10^{-4}\ cm^{-1}$) consistent with the monoclinic space group $C2/c$, and an elongated rhombic CuN_6 chromophore stereochemistry.

The powder ESR spectrum of the $Cu/Zn(C_5H_5NO)_6(ClO_4)_2$ system [83] at room temperature shows a clear anisotropic signal $g_\parallel = 2.367$ ($A_\parallel = 103 \times 10^{-4}\ cm^{-1}$), $g_\perp = 2.080$ ($A_\perp = 9 \times 10^{-4}\ cm^{-1}$) with an additional isotropic signal at 2.183 displaying no hyperfine structure. The anisotropic signal is temperature invariant and the single-crystal rotation spectra are consistent with three (see Fig. 5(a)(ii)) magnetically inequivalent sites with equivalent g-factors related by the trigonal three-fold axis. The isotropic signal shows some evidence of splitting at low temperature, suggestive of a dynamic Jahn-Teller site, but the whole system is complicated by the presence of weak ESR signals (<16%) due to impurity solvated species, in this system such as $Cu(C_5H_5NO)_4(ClO_4)_2$, solvate.

The effect of temperature on the powder ESR spectra [102] of Cu/Zn-(tetramethylene sulphoxide)$_6(ClO_4)_2$ and Cu/Zn(N-methylimidazole)$_6(ClO_4)_2$ changes an anisotropic ESR signal at room temperature without copper hyperfine structure to an anisotropic signal at 95 K (Table 4) with hyperfine on the highest g-value only, suggesting a fluxional Jahn-Teller effect at room temperature, changing to a static elongated CuL_6 chromophore at 95 K. The single-crystal ESR spectrum of $Cu/Zn(imidazole)_6Cl_2 \cdot 4\ H_2O$ [103] also shows an isotropic powder ESR spectrum at room temperature $g_i = 2.1702$ ($A_i = 57.67 \times 10^{-4}\ cm^{-1}$) becoming anisotropic at 77 K, $g_\parallel = 2.2995$ ($A = 158.3 \times 10^{-4}\ cm^{-1}$) and $g_\perp = 2.0878$ ($A = 37.5 \times 10^{-4}\ cm^{-1}$) again suggestive of a near dynamic to static Jahn-Teller change with temperature. As the space group of $Zn(HZDT)_6Cl_2 \cdot 4\ H_2O$ is triclinic $P\bar{1}$ [104], at room temperature only one orientation of the three possible magnetic sites is observed, which is indicative of tunneling between the three Jahn-Teller configurations, which is justified by the observation of some anomalous angular dependence of the g-factors.

The first clear evidence of the temperature variability of the ESR parameters for the copper(II) ion was for the triclinic copper doped $Ba_2Zn(HCO_2)_6 \cdot 4\ H_2O$ [105] system (Table 13) but interpreted in terms of a

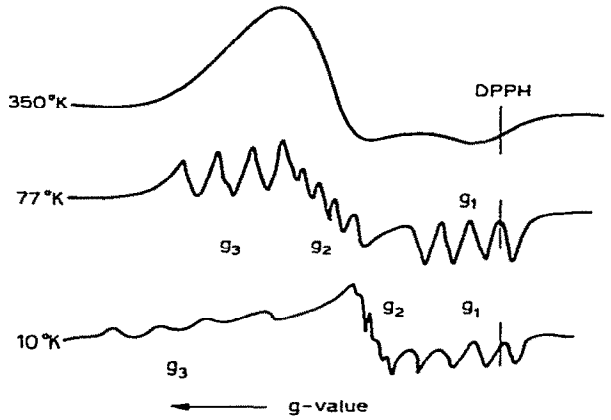

Fig. 14. The powder ESR spectra of copper doped $K_2Zn(H_2O)_6(SO_4)_2$. Reproduced by permission of the authors [101].

vibronic mixing of the $3d_{z^2}$ level of the copper(II) ion into the $3d_{x^2-y^2}$ ground state. In the single-crystal measurements a maximum of four lines were observed in any one direction, which coalesced into a single line, in the direction of the lowest g-factor, a behaviour that is consistent with the presence of only one magnetic site as expected for a triclinic space group.

The most important work [101] in this area is that of the copper doped $K_2Zn(OH_2)_6(SO_4)_2$ system which first established the temperature variability of the ESR spectra down to liquid helium (Fig. 14) and then interpreted the temperature variability in terms of the dynamic Jahn-Teller effect using a potential energy diagram comparable to Fig. 3(c)(i) and first suggested a potential energy barrier between two misaligned elongated chromophores. Not only

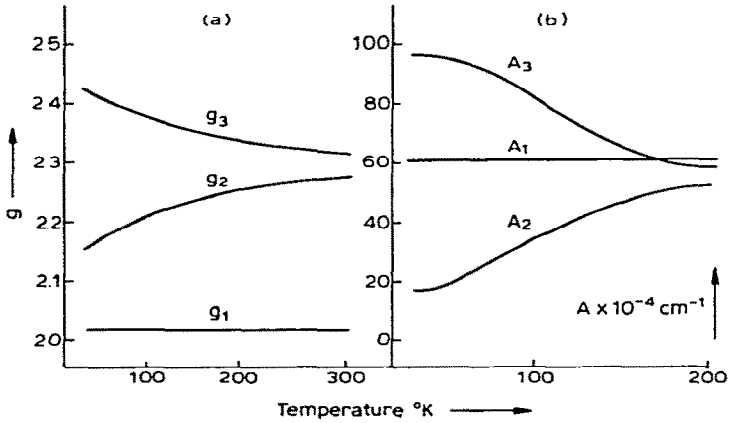

Fig. 15. Copper doped $K_2Zn(OH_2)_6(SO_4)_2$. Temperature variation of (a) the g-factors and (b) the A-values, single crystal data. Reproduced by permission of the authors [101].

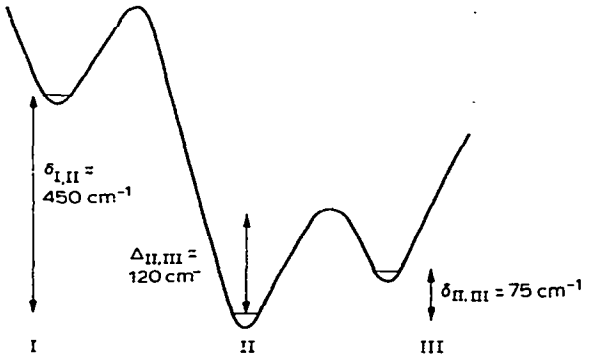

Fig. 16. Circular cross section of the potential energy surface associated with the three Jahn-Teller Wells I—III in copper doped $K_2Zn(OH_2)_6(SO_4)_2$. Reproduced by permission of the authors [101].

did the data illustrate the temperature variation of the *g*-factors, but also of the *A*-factors (Fig. 15) which display the same type of temperature variation characteristic of the *g*-values, namely, that A_3 increases with decreasing temperature, A_2 decreases and A_1 is temperature invariant. The single-crystal spectra showed two sets of four hyperfine lines which coalesced into one set of four lines along the *b*-axis and in the *ac*-plane of the monoclinic crystal, consistent with the presence of two misaligned CuO_6 chromophores in the $P2_1/a$ unit cell. The directions of the *g*-factors of the individual sites corresponded with the direction of the Cu—O bonds and the direction of the *g*-factors are shown to be temperature invariant as required by the dynamic Jahn-Teller effect. From a quantitative analysis of the temperature variation of the *g*- and *A*-factors, the energy splitting values from the three wells (Fig. 16) were found to be $\delta_{II,III} = 75$ cm^{-1} and $\delta_{II,I} \simeq 450$ cm^{-1}. The rate of inter-well jumping between the two lowest valleys was determined from the temperature variation of the line widths and yielded a $\Delta_{II,III}$ value of $\sim$120 cm^{-1} for the height of the warping barrier between Wells II and III. In view of the detailed energy data concerning the barrier heights of Fig. 16, it must be emphasised that the data were obtained in the copper doped potassium Tutton salt. It would be of interest to examine the data from the corresponding copper doped ammonium and caesium Tutton salts, firstly, to see how these varied with the different cations and secondly, to see how the values compared with the extent of fluxional behaviour indicated by the variable temperature X-ray crystallography results [31,32] of section C and illustrated in Fig. 6. An equivalent but less detailed analysis of the single-crystal ESR spectrum [106] of the $Cu/Mg(OH_2)_6H_2$edta complex has also been reported.

The term fluxional [14] was first introduced to account for the temperature variation of the *g*- and *A*-factors of the $Cu/Zn(hfacac)_2py_2$ [86] system down to liquid helium temperatures. Down to 133 K only one magnetic site existed, displaying marked temperature variability with *g*-factors typical of a fluxional elongated rhombic octahedral CuN_2O_4 chromophore (Table 13).

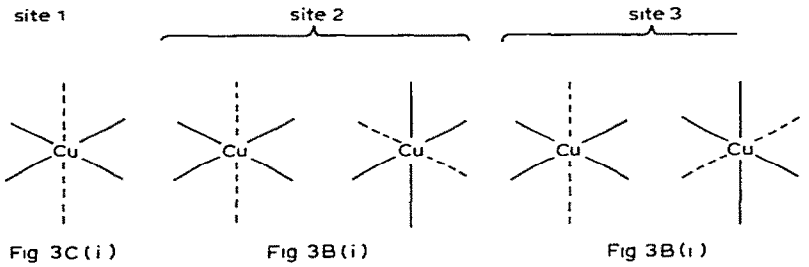

Fig. 17. The CuN_2O_4 chromophore stereochemistries contributing to the three non-equivalent magnetic sites of copper doped $Zn(hfacac)_2py_2$.

Below 133 K more than one magnetic site is present: at 4.2 K the high temperature site is still present and the most intense, but in addition two further equivalent sites are present, with the two sites related by the two fold axis of the zinc host lattice. The g-factors are clearly different from the high temperature spectrum with ($g_1 = 2.074$, $g_2 = 2.226$ and $g_3 = 2.242$). These pseudo compressed type g-factors suggest a pseudo compressed type doped CuN_2O_4 chromophore stereochemistry, which contrasts with the elongated stereochemistry associated with the most intense magnetic site and for the pure complex (Table 12). The three magnetic sites are misaligned by ca. 90° (as required by trapping out of a pseudo dynamic near cubic system) and only one of them is elongated (Fig. 3(c)(i)) and fluxional, while the other two are pseudo-compressed (Fig. 3(b)(i)), with near equivalence of the two contributing 90° misaligned elongated rhombic octahedral CuN_2O_6 chromophores (Fig. 17) at each of sites (2) and (3).

The higher accuracy with which the g- and A-factors of copper doped zinc complexes may be measured is well illustrated in the powder ESR spectra of a series of $Cu/Zn(dien)_2XY$ complexes [61], Table 14, all involving on axial elongated type of spectra, which becomes more axial with decreasing tem-

TABLE 14

ΔA_3-values (%) for $Cu/Zn(dien)_2XY$ complexes

X	Y	ΔA_3 (%)
Cl	ClO_4	8.9
Cl	BF_4	10.1
Cl	Cl, H_2O	17.8
Br	Br, H_2O	22.0
NO_3	NO_3 (monoclinic)	8.8
I	I	29.5
Cl	NO_3	31.4
Br	NO_3	36.0

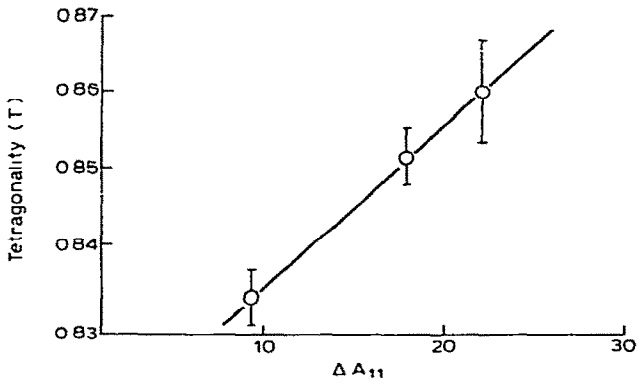

Fig. 18. The tetragonality (T) of $Cu(dien)_2XY$ complexes v. $\Delta A_{\parallel}$% measured on the corresponding copper doped $Zn(dien)_2XY$ powder ESR spectra.

perature; the single-crystal data for the copper doped $Zn(dien)_2Br_2 \cdot H_2O$ system [87], clearly indicates the characteristic temperature variation (see Fig. 15), of a fluxional CuN_6 chromophore. If ΔA_3, the percentage change in A_3 from room temperature to liquid nitrogen temperature, is taken as a measure of the extent of fluxional behaviour, there is a significant variation in the ΔA_3 values (8.9—36.0%) depending on the nature of the anions X and Y (Table 14) the increasing value of which suggests an increasing amount of fluxional behaviour. If the ΔA_3 values of the three complexes of known crystal structure are plotted against their tetragonalities (Fig. 18) a reasonable correlation is obtained [61] which suggests that the small differences in the observed tetragonalities 0.83—0.86, are real and reflect a difference in the fluxional behaviour of the $Cu(dien)_2^{2+}$ cation in these crystal lattices. It also suggests that in this series of near isostructural $M(dien)_2XY$ complexes, there is a correlation between the electronic properties of the concentrated and dilute complexes, not withstanding that the ZnN_6 chromophore stereochemistry of the host lattice has a compressed rhombic octahedral stereochemistry (XVI) [61], compared with the elongated rhombic stereochemistry of the pure copper(II) complex (Table 12).

The room temperature ESR spectrum of the copper doped $Zn(C_5H_4NSO_3)_2 \cdot 4\ H_2O$ system [107] (Table 13) was one of the earliest spectra [108] to be reported as indicating a compressed rhombic octahedral stereochemistry, but which indicated an elongated stereochemistry in the corresponding pure copper(II) complex (2.059, 2.080 and 2.294); both predictions were made in the absence of any crystallographic data on the structure of the MO_4N_2 chromophore in either the zinc or copper complexes. The crystal structures [107] of $Zn(C_5H_4NSO_3)_2 \cdot 4\ H_2O$ and $Cu(C_5H_4NSO_3)_2 \cdot 2\ H_2O$ (Table 12) are now known; both are monoclinic, but they are not isomorphous as their formulae suggest, but both involve a *trans* MO_4N_2 chromophore. In the zinc complex the ZnO_4N_2 chromophore has a compressed rhombic octahedral

stereochemistry, seemingly consistent with the room temperature g-factors (Table 13) with an R-value of 2.64. In the copper(II) complex the CuO_4N_2 chromophore is elongated rhombic octahedral with g-factors (Table 13) yielding an R-value of 0.20, consistent with the elongated CuO_4N_2 chromophore. Nevertheless the g-factors of copper doped $Zn(C_5H_4NSO_3)_2 \cdot 4\ H_2O$ are clearly temperature variable [107] (Table 13), consistent with the presence of marked fluxional behaviour, with the R-value changing from 2.64 to 0.41 suggesting an elongated stereochemistry at the low temperature typical of a fluxional CuN_2O_4 system. This system emphasises the dangers of attempting to predict the CuL_6 chromophore stereochemistry in Cu/Zn doped systems in the absence of structural data and the effect of temperature on the ESR spectra.

The powder ESR spectra [109] of copper doped $Zn(methoxyacetate)_2 \cdot 2\ H_2O$ (XVIII), (Table 13) is of interest as it is anisotropic even at room tem-

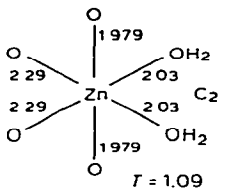

(XVIII) $Zn(methoxyacetate)_2 \cdot 2\ H_2O$

perature, with a reversed type ESR spectrum, $g_\perp > g_\parallel > 2.0$, and suggests a compressed CuO_6 chromophore stereochemistry, an observation that would not be inconsistent with the compressed rhombic octahedral stereochemistry of the corresponding $Cu(methoxyacetate)_2 \cdot 2\ H_2O$ complex [40,47] except that the zinc(II) complex (XVIII) [109] is not isomorphous with the copper-(II) complex (IX), (orthorhombic $Fdd2$ and monoclinic $P2_1/n$, respectively) despite their comparable stoichiometry. In addition while the methoxyacetate chelate ligands of the copper(II) complex (IX) occupy *trans*-planar positions about the centrosymmetric CuO_6 chromophore; in the zinc complex (XVIII) the arrangement is *cis*-octahedral, with a *cis* elongated distortion, involving a 2-fold site symmetry at the zinc atom. The powder ESR spectrum (Table 13) is axial with little evidence for a rhombic component and with clear evidence for the largest copper hyperfine splitting on the lowest $g_\parallel$-factor, but none on the higher $g_\perp$, a pattern that is more typical of an ESR spectrum consistent with a genuine compressed octahedral stereochemistry (see section H). In addition the spectrum shows little change with temperature.

The doped ESR spectrum reported [110] for copper doped $Zn(NH_4)_2(NH_3)_2(CrO_4)_2$ (Table 13) is nearly axial with an R-value of 14.3, well above 1.0 and a very low lowest g-factor of 2.017 at room temperature, values that clearly suggest a compressed axial CuN_2O_4 chromophore with only a small rhombic component. The lowest g_1-factor of 2.017 would seem to rule out a pseudo compressed rhombic octahedral stereochemistry and the associated largest A-factor of $144.6 \times 10^{-4}\ cm^{-1}$ further supports a genuine static com-

pressed rhombic octahedral CuN_2O_3 stereochemistry. Nevertheless the ESR spectrum at 77 K, $g_1 = 2.014$, $g_2 = 2.109$ and $g_3 = 2.287$, suggests a compressed rhombic octahedral stereochemistry, as the lowest g-factor is temperature invariant, with the temperature variability restricted to g_2 decreasing and g_3 increasing at the lower temperature. This pattern is difficult to rationalise with any sort of fluxional behaviour even including two compressed rhombic octahedral chromophores misaligned by 90°, but this possibility seems to be ruled out by the non temperature variable and almost free electron g-value of the lowest g-factor. A two dimensional fluxional behaviour between two very rhombic compressed CuN_2O_4 chromophores with the compression axes aligned parallel, to retain the lowest g-factor may be possible, but the realisation that the reported ESR spectra are not continuously variable from 295—77 K, but are characterised by a sharp transition at 278 K and are then virtually temperature independent down to 77 K, indicates a phase change at 278 K and rules out any fluxional behaviour in this system. The pattern of g-factors at low temperature suggests a transition to a distorted trigonal bipyramidal CuN_2O_2O' chromophore [64,111,112] or alternatively a *cis*-distorted octahedral $CuN_2O_2O_2'$ chromophore [113].

Type C(ii) concentrated and dilute

The non-temperature variable ESR spectra of the vast majority of copper(II) complexes with an elongated tetragonal octahedral stereochemistry [2,3] are typical of Fig. 3(c)(ii) behaviour with $B > kT$, and are not reported in detail.

An interesting set of ESR spectra is reported (Fig. 19) for <1% copper doped Zn(pyrazine)$SO_4 \cdot 3\ H_2O$ [114], which crystallises in the triclinic space group $P\bar{1}$ with $Z = 1$. Three g-values are observed with copper hyperfine on the highest and lowest (Table 6) and the angular variations are consistent with three magnetically equivalent sites, with comparable intensity and equivalent rhombic g-factors, $g_3 = 2.414$, $g_2 = 2.214$ and $g_1 = 2.109$, which equate with an elongated rhombic octahedral CuO_6 chromophore. As the spectra are reported to be non-temperature variable they would seem to represent the three static potential wells of Fig. 3(a)(ii) all equally occupied with the elongation axes misaligned by 90°, but exhibiting no fluxional behaviour as B is greater than thermal energy.

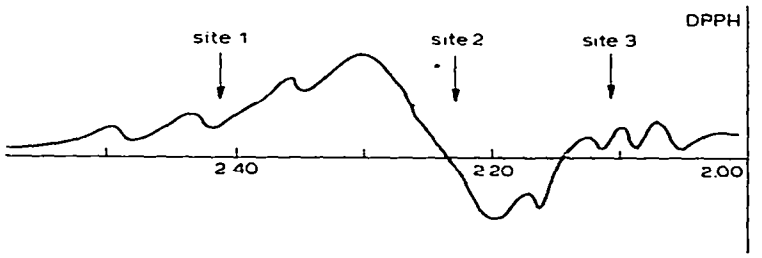

Fig. 19. The single-crystal ESR spectrum of ca. 1% copper doped Zn(pyrazine)$(SO_4) \cdot 3\ H_2O$ Reproduced by permission of the author [114].

(ii) Summary

This ESR section illustrates not only the varying behaviour of the different pure copper(II) complexes and different copper(II) doped zinc(II) systems and their variation with temperature, but occasionally the different behaviour of the concentrated copper(II) complexes and their related copper-(II) doped systems [107] and emphasises the importance of co-operative effects [13,20] in these molecular type lattices of concentrated copper(II) complexes compared with the electronic properties of isolated copper(II) chromophores in the corresponding doped systems.

F. ELECTRONIC SPECTRA

Figure 20 gives a section [24] through the potential energy surface of Fig. 1(a) and shows the splitting of the ^2E_g term into two components, $\psi_-\psi_+$, with no appreciable splitting of the higher energy $^2T_{2g}$ term. Two transitions are predicted, E_1 and E_2, for $E_{JT} >> h_\delta > kT$, and application of the Frank-Condon principle, within the harmonic first order model, gives $E_1 \simeq 4E_{JT}$ and $E_2 \approx \Delta + 2E_{JT}$. Table 15 lists a number of copper(II) complexes containing CuN_6 chromophores with equivalent ligands and gives, d_0, the average Cu—N distance, the Jahn-Teller radius, R_{JT}, calculated [24] from the expression $R_{JT}^2 = \Sigma_{i=1}^6 \Delta d_i^2$, the value of E_{JT} calculated assuming $E_1 = 4E_{JT}$, E_2 and f, the quadratic force constant calculated from $f = 2E_{JT}/R_{JT}^2$. The values of E_2 are reasonably constant irrespective of whether a dynamic or static system is

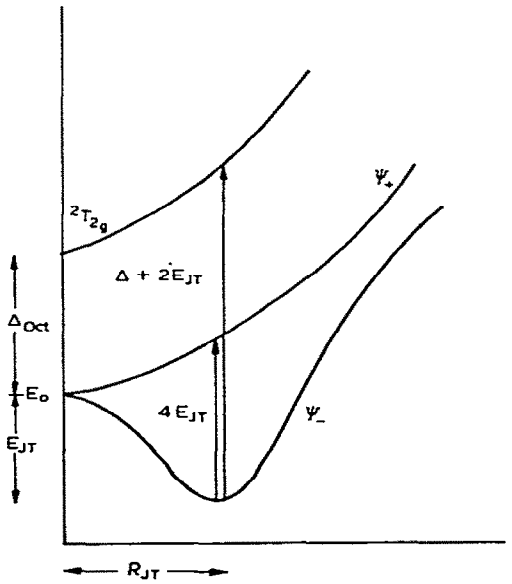

Fig. 20. A section through the potential energy surfaces of the Mexican Hat of Fig. 1(a). Reproduced by permission of the authors [24].

TABLE 15

Structural and spectroscopic data for some copper(II) complexes involving equivalent ligands at room temperature. Reproduced by permission of the authors [24].

Compound	d_0(Å)	R_{JT}(Å)	E_{JT}(kK)	E_2(kK)	$f = 2E_{JT}/R_{JT}^2$ (mdyn Å^{-1})
Dynamic					
$Cu(en)_3SO_4$	2.150	0.358	2.18	15.7	0.68
$K_2PbCu(NO_2)_6$	2.111	0.333	1.75	16.5	0.63
$Tl_2PbCu(NO_2)_6$	2.118	0.308	1.86	16.5	(0.78)
$Cu(tach)_2(NO_3)_2$	2.164	0.329			0.80
Pseudo dynamic					
$Rb_2PbCu(NO_2)_6$	2.136	0.252	1.92	15.7	1.20
$Cs_2PbCu(NO_2)_6$	2.171	0.343	1.92	16.3	(0.75)
Static					
$K_2CaCu(NO_2)_6$	2.138	0.303	1.98	16.5	0.85
$K_2SrCu(NO_2)_6$	2.127	0.318	1.90	16.5	0.75
$K_2BaCu(NO_2)_6$	2.132	0.308	1.92	16.55	0.81
$Cu(bipy)_3(ClO_4)_2$	2.134	0.355	2.17	15.4	0.69
$Cu(phen)_3(ClO_4)_2$	2.134	0.336	1.90	15.2	0.67

involved and the values of E_{JT} appear significantly lower in the dynamic Jahn-Teller system, than in the static systems of the $M_2^I M^{II} Cu(NO_2)_6$ complexes, with the pseudo dynamic complexes equating better with the static systems, consistent with the interpretation of their structures as involving a pseudo compressed octahedral stereochemistry. The differences do seem to correlate in the hexanitro complexes [24], with the d_0 values (the average Cu—N distances), but even here the value for $Rb_2PbCu(NO_2)_6$ does seem rather high for no good reason. As the d_0 values are constant, then it is not surprising that the R_{JT} values are reasonably constant, as both are calculated from the Cu—N distances. At present there are too few reliable data for the chelate nitrogen systems [21] of Table 15 to indicate a definite correlation with hexanitro complexes, but the structural and spectroscopic data are of the same order of magnitude, if not showing a 1 : 1 correlation, with probably least correlation observed in the quadratic force constants, f, which are evaluated as a ratio of the spectroscopic and structural data, $f = 2E_{JT}/R_{JT}^2$.

The use of polarised single-crystal spectroscopy in these fluxional systems has not been extensive: all the cubic systems [68] show no polarisation and the trigonal [77,115] only show a change of intensity (Fig. 21(a)) which is in marked contrast to the type of polarisation obtained in a statically distorted system such as $K_2BaCu(NO_2)_6$ [116] (Fig. 21(b)) or $Cu(bipy)_3(ClO_4)_2$ [71]. The observation of no polarisation, but only a change in intensity could be used to suggest the presence of extensive fluxional behaviour, in concentrated copper(II) complexes, such as $[C_{14}H_{19}N_2]Cu(hfacac)_3$ [71]. Neverthe-

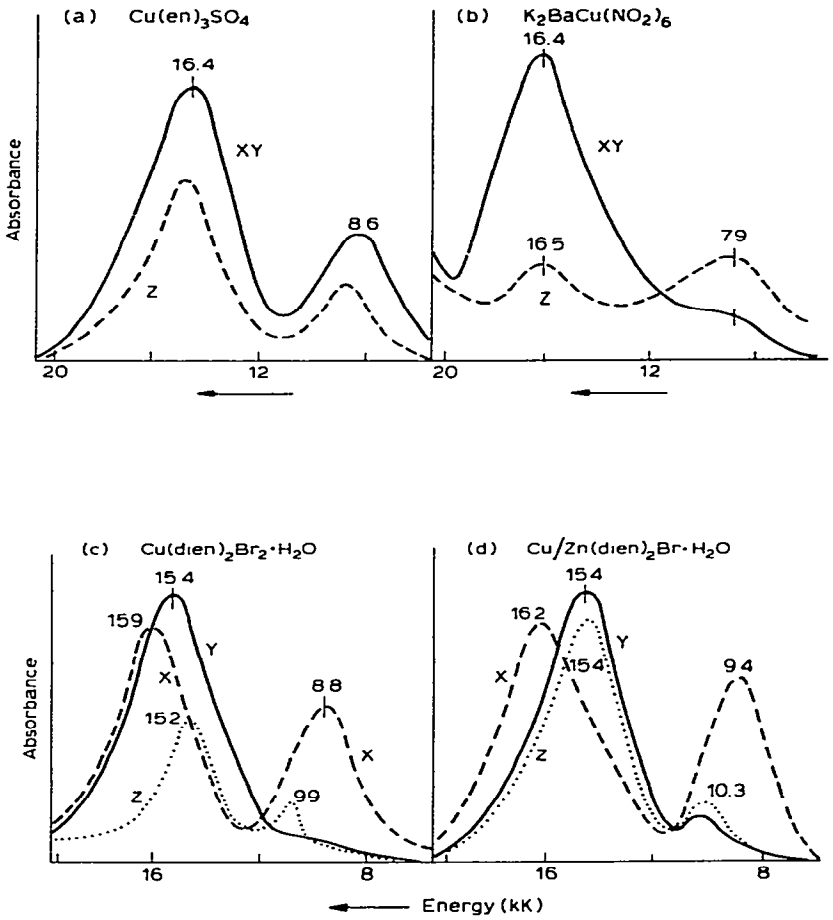

Fig. 21. The polarised single-crystal electronic spectra.

less it should be remembered that the presence of a small amount of fluxional behaviour does not rule out the observation of marked polarisation, as in $Cu(dien)_2Br_2 \cdot H_2O$ [117] or $Cu/Zn(dien)_2Br_2 \cdot H_2O$ [61] (Fig. 21(c) and (d)) both of which involve weak fluxional behaviour.

Some attempts have been made to predict the stereochemistry [13,59] of the CuL_6 chromophore doped in a diamagnetic host lattice, i.e. 10—30% copper doped Ba_2ZnF_6, from the electronic reflectance spectra, but the final answer even to this question must await the availability of X-ray crystallographic data on 5—10% copper doped zinc systems [61,107,118].

Finally the lack of effect of temperature on the electronic energies of fluxional copper(II) systems must be mentioned: as electronic transitions are very fast, the observed spectra represent the extremes of the CuL_6 chromophore stereochemistry. As these represent the distorted environment in which

the chromophore spends most of its time and as this is not affected by the extent of thermal mixing, the electronic spectra of fluxional systems are essentially temperature independent, unless the stereochemistry happens to change with temperature in the event of a phase transition. Thus although the electronic spectra yield the electronic energies of fluxional systems, they are much less informative of fluxional behaviour than the ESR spectra.

G. JAHN-TELLER EFFECTS

(i) Cooperative

The three types of behaviour of copper(II) complexes described by Fig. 3((a)—(c)) must largely be determined by hydrogen bonding and Van der Waals forces, which together make up the lattice packing effects which determine a given space group structure. Due to the ability of the d^9 configuration of the copper(II) ion to accommodate small differences of bond lengths and bond angles, a flexible stereochemistry [4] or plasticity effect [5] results and copper(II) complexes are characterised [2,3] by a range of distorted rather than regular stereochemistries. A converse of this flexible stereochemistry is that in concentrated copper(II) complexes, the presence of adjacent CuL_6 chromophores may also influence the final copper(II) stereochemistry and this is referred to as the cooperative Jahn-Teller effect [13]. This is particularly important where bridging monoatomic ligands common to two adjacent chromophores are present, as in K_2CuF_4, [33,59,60] but is also important for more molecular lattices [13] involving isolated anions, such as $Cu(NO_2)_6^{4-}$ in the $M_2^{I}M^{II}Cu(NO_2)_6$ complexes, or cations such as $Cu(dien)_2^{2+}$ in $Cu(dien)_2X_2$ complexes [61]. For the formation of a dynamic Jahn-Teller situation, Fig. 3(a)(i), not only must six equivalent ligands be present, but the complex must crystallise in a high symmetry lattice, cubic or trigonal, for the maximum cooperative Jahn-Teller effect to occur. The change to lower symmetry systems, two dimensional fluxional or static, invariably results in a change in phase, i.e. cubic to orthorhombic in the hexanitro series (Table 8) which is accompanied by a change from an isotropic to anisotropic ESR spectrum, but very little change in the Jahn-Teller radius R_{JT} or Jahn-Teller energy E_{JT} is observed, Table 15. This suggests that the cooperative Jahn-Teller effect [13] present in all of these concentrated copper(II) complexes are comparable and only modified slightly by the symmetry of the lattice. The situation in copper doped diamagnetic host lattices is, however, different as at low dilution the copper—copper separations are sufficiently large to rule out any cooperative effects between the copper chromophores and the differences observed [85] in the ESR spectra of $Cu(phen)_3(NO_3)_2 \cdot 2H_2O$ (one magnetic centre) and copper doped $Zn(phen)_3(NO_3)_2 \cdot 2H_2O$ (two 90° misaligned magnetic centres) are good examples of the cooperative Jahn-Teller effect. In the 1—100% copper doped Ba_2ZnWO_6 system [13] (Fig. 22(a)) the reflectance spectra are very dependent on the percentage doping, but as these differen-

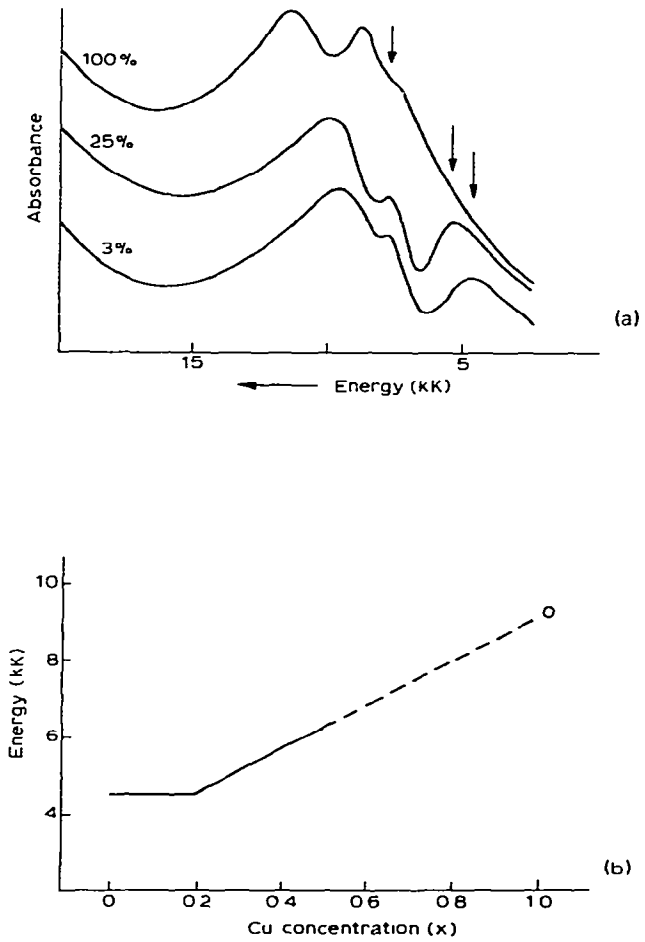

Fig. 22. The electronic reflectance spectra of 1—100% Cu/Ba_2ZnWO_6; (a) variation with composition, (b) the variation of the $d_{z^2} \leftarrow d_{x^2-y^2}$ transition (↓), $4E_{JT}$, with composition x. Reproduced by permission of the authors [13].

ces are accompanied by a change of phase, cubic to tetragonal, the changes of Fig. 22 cannot be associated only with a change in the cooperative Jahn-Teller effect, although the change in energy of the $d_{z^2} \rightarrow d_{x^2-y^2}$ transition from 4.5 → 6.5 kK for the doping range 20—50% does seem to be associated with this effect in this system.

(ii) Non-cooperative

Nevertheless for a number of coordination complexes [67] of the copper-(II) and zinc(II) ions, which have the same empirical formula and the same space group, no change in phase occurs over the range 1—100% copper doped

TABLE 16

Space group data, stereochemistry, electronic spectra and g- and A-factors for 100% and 1% copper for five isomorphous copper(II) and zinc(II) complexes [67]

No.	Complex	Space group	Copper(II)				Zinc(II)			
			a	b	c	$\beta°$	a	b	c	$\beta°$
1	$M(bipyam)_2(ClO_4)_2$	$C2/c$	9.35	12.88	19.69	102.8	9.39	13.03	19.80	104.3
2	$M(dien)_2Br_2 \cdot H_2O$	$P2_1/c$	13.90	8.91	14.21	101.9	13.81	8.91	14.28	101.23
3	$M(dien)(bipyam)(NO_3)_2$	$P2_1/c$	12.20	16.00	9.85	91.0	12.34	16.26	9.92	92.0
4	$M(bipy)_2(ONO)(NO_3)$	$P2_1/n$	15.39	12.06	11.10	99.2	15.49	11.93	11.27	101.2
5	$M(py)_3(NO_3)_2$	$C2/c$	12.78	9.20	16.06	108.35	12.60	9.40	16.27	108.9

	Stereochemistry	*Electronic spectra ($\times 10^{-3}$ cm^{-1})*		
1	Compressed tetrahedral	16.3	13.0 sh	10.6
2	Elongated rhombic octahedral	15.9		9.5
3	Square pyramidal	15.0 sh	13.0	
4	*Cis*-distorted octahedral	14.8		9.3
5	Trigonal bipyramidal	13.0 sh	12.2	10.5 sh

	100% Cu			*1% Cu-doped zinc*					
	g_1	g_2	g_3	g_1	g_2	g_3	A_1	A_2	A_3
1	2.059	2.069	2.244	2.058	2.069	2.244			145
2	2.043	2.098	2.233	2.043	2.100	2.204	ca. 25	50.9	127.3
3	Misaligned			2.026	2.110	2.220	43.3	66.2	148.5
4	2.027	2.17	2.205	2.025	2.165	2.196	ca. 25	101	112
5	2.025	2.166	2.266	2.026	2.190	2.252	68.5	55.6	89.0

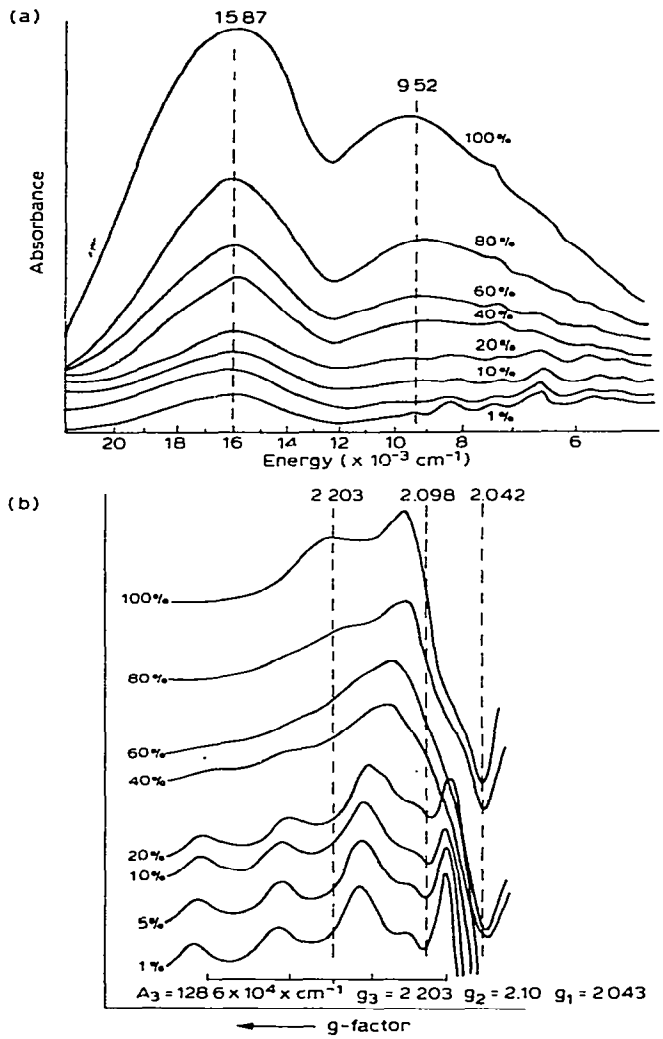

Fig. 23. (a) The electronic reflectance spectra of 1—100% copper doped $Zn(dien)_2Br_2 \cdot H_2O$. (b) The polycrystalline ESR spectra of 1—100% copper doped $Zn(dien)_2Br_2 \cdot H_2O$.

zinc complex, Table 16; for these five different stereochemistries (Table 16) there is no significant change in electronic reflectance or ESR spectra from 1—100% (Table 16), which is illustrated for one complex in Fig. 23.

Thus the data of Table 16 show no significant variation of either the *g*-factors or the electronic transitions, over the complete concentration range 1—100%, and strongly suggest that the stereochemistry of the CuL_n chromophore in these soft molecular lattices is independent of the percentage copper

concentration, for a wide range of different stereochemistries. This implies that while for each of these pure copper(II) complexes the actual stereochemistry must be determined by a number of factors, i.e. the type and number of ligands present, the non-spherical symmetry of the copper(II) ion, crystal lattice effects such as hydrogen bonding and Van der Waal forces, the stereochemistry is not determined by the presence of the other copper(II) complexes in the lattice as would be required by the cooperative Jahn-Teller effect [13]. In addition as the stereochemistry of the CuL_n chromophore is the same for 100% Cu and 1%, in the latter, the CuL_n stereochemistry must be independent of the pure ZnL_n chromophore stereochemistry [66], an independence that is best seen in the constancy of the electronic reflectance spectra (Fig. 23(a)). Consequently, in these systems, it would be valid to use the more accurately measured g- and A-factors of the 1% copper(II)-doped zinc(II) complexes, with the CuL_n chromophore stereochemistry of the 100% copper(II) complex, but it must be emphasised that before this type of extrapolation may be used the following conditions must be fulfilled; namely, (a) the copper(II) and zinc(II) complexes have the same composition and space group with comparable unit cell parameters, and (b) the g-factors and electronic spectra must be independent of the copper concentration; only then can these complexes be described as non-cooperative Jahn-Teller systems.

The first prediction [119] of the non-cooperative Jahn-Teller effect was the equivalence of the g-factors [94] of $(NH_4)_2Cu(OH_2)_6(SO_4)_2$ and of copper doped $(ND_4)_2Zn(OH_2)_6(SO_4)_2$ [119].

H. COMPRESSED OCTAHEDRAL STEREOCHEMISTRY

While the bulk of this article has reviewed the fluxional properties of copper(II) complexes in the process it has cast increasing doubt [12,13,87] on the existence of a genuine compressed rhombic octahedral stereochemistry for a CuL_6 chromophore in concentrated copper(II) complexes.

The compressed stereochemistries of $Rb_2PbCu(NO_2)_6$, $Cs_2PbCu(NO_2)_6$ (I), $Cu(dien)_2(NO_3)_2$ (II), K_2CuF_4 (XIV), Ba_2CuF_6 (XV) and Cu(methoxyacetate)$_2$ 2 H_2O (IX) all have alternative descriptions. The compressed axial structure [120] of β-$Cu(NH_3)_2Br_2$ (Table 12) was only based on X-ray powder data and that of $Cu(NH_3)_2C_2O_4 \cdot 2\ H_2O$ [121] (Table 12) is not consistent with the single crystal ESR data. The structure of $Cu(fomp)_2(meen)$ [122] (Table 12) could well be a genuine static compressed rhombic octahedral stereochemistry, but as an unusually complicated thermal motion was involved and as no ESR spectra were reported, the final answer must await temperature variable ESR spectra and preferably a low temperature crystal structure determination.

The ESR evidence [12,123] for a compressed rhombic octahedral stereochemistry in copper(II) doped systems is much more convincing; see Table 17. All of these systems are characterised by low g-values, of approximately 2.00, combined with significant copper hyperfine splitting on the lowest g-factors characteristic of a d_{z^2} ground state and generally considered to arise [2,123]

TABLE 17

Some typical examples of Cu doped systems involving possible compressed rhombic octahedral CuL_6 chromophores

Complex	g_1	g_2	g_3	A_1	A_2	A_3	Ref.
$A_1 >> A_2 \approx A_3$							
$ZnWO_4$	2.000	2.379	2.434	77	18		124
CsCl	2.012	2.217	2.217	151			125
NH_4Cl(II)	2.000	2.219		233	67		126
NH_4Br(I)	2.004	2.217	2.217	182			127
Ba_2ZnF_6	1.990	2.360		125			13
$(NH_4)_2Zn(NH_3)_2(CrO_4)_2$	2.017	2.216	2.230	147	10	10	110
$Cu(NH_3)_2Cl_2/NH_4Cl$	2.000	2.223		228	65		127
$Cu(NH_3)_2Cl_2/NH_4Cl$	2.008	2.178		144			123
5% Cu/Zn(methoxyacetate)$_2 \cdot 2\,H_2O$	2.077	2.328		110			109
2% Cu/Cd(pyrazole)$_2Cl_2$	2.01	2.21	2.24	130			128
$A_1 < A_2 < A_3$							
5% Cu/Zn(bipyam)$_2(NO_3)_2$	2.030	2.194	2.216	52	82	84	57
Cu/Zn(bipy)$_2$(ONO)NO_3	2.024	2.168	2.199	30	92	106	85, 57
Cu/Zn(bipyam)$_2$(ONO)NO_2	2.028	2.170	2.203	32	94	96.4	76
Cu/$[Zn_{3.5}O(O_2CMe)_5(py)]_2$	1.996	2.267	2.293	18.3	32.5	164.4	129

from symmetry mixing of the $3d_{z^2}$ and $4s$ orbitals. The spectra show little temperature variation and must therefore relate to an essentially static CuL_n stereochemistry which could well be compressed six coordinate octahedral, but in the static doped systems the possibility of a *cis* distorted octahedral CuL_6 chromophore [130,131] as in the copper doped Zn(methoxyacetate)$_2 \cdot 2\,H_2O$ (XVIII) [109], where the ZnO_6 chromophore is *cis*-distorted octahedral, should not be ruled out. Likewise in these copper(II) doped systems a change in coordination number is possible, i.e. six to five as suggested for the low temperature g-factors of the copper doped $Zn(NH_3)_2(NH_4)_2(CrO_4)_2$ [110] (see section E).

Consequently in view of the doubt about the existence of the static compressed tetragonal octahedral stereochemistry in concentrated copper(II) complexes, it is not possible to suggest an "electronic criterion" for this stereochemistry [132], but there may well be an ESR criterion [123] in the dilute copper systems.

I. CONCLUSIONS

(a) From the limited number of room temperature and low temperature crystal structures that have been determined the structural changes are con-

sistent with the warped Mexican hat model for the potential energy surface for these dynamic → static changes in copper(II) complexes.

(b) In these dynamic—static changes the phase transitions involve very low energies (ca. 0.1 kcal $mole^{-1}$) and the average structural (d_0 and R_{JT}) and spectroscopic (E_{JT}, E_2 and f) properties show little variation across the phase transitions.

(c) A number of systems involve a two dimensional dynamic situation midway between dynamic and static and characterised by a pseudo compressed octahedral stereochemistry and pseudo reversed type g-factors with $g_\perp > g_\parallel > 2.0$. In these complexes the compressed octahedral stereochemistry is not a genuine static stereochemistry of the copper(II) ion, but a two dimensional time average (or static disordered) structure comparable to the three dimensional time average structures of the regular octahedral and trigonal octahedral stereochemistry of copper(II) complexes.

(d) While the bulk of the elongated rhombic octahedral complexes of the copper(II) ion involve a static CuL_6 chromophore stereochemistry, with tetragonalities $T = 0.8$—0.85, an increasing number, characterised by tetragonalities > 0.85, are found to have temperature variable or fluxional stereochemistry, in which T decreases with decreasing temperature. These fluxional systems are also characterised by a variation of the local molecular g-factors such that the highest, g_3 increases, g_2 decreases and the lowest g_1 remains temperature invariant. At room temperature the R-value, $g_2 - g_1/g_3 - g_2$, is >1.0 suggesting an approximate d_{z^2} ground state, but at low temperature the R-value decreases to <1.0, consistent with an approximate $d_{x^2-y^2}$ ground state. Consequently the g-factors of these fluxional systems are of little value in suggesting the local CuL_6 chromophore stereochemistry unless they are first checked for non-temperature variability. By the same criteria, g-factors of fluxional copper(II) complexes cannot be involved in calculating the molecular orbital coefficients of the CuL_6 chromophore as the usual molecular orbital expressions refer to static stereochemistries.

(e) The importance of cooperative lattice effects in pure copper(II) complexes relative to the copper(II) doped/zinc(II) complexes is becoming increasingly apparent, especially those involving rigid lattices, where the change in phase associated with a high symmetry to low symmetry transition, can result in a change in the electronic properties, but usually these are small. In copper doped diamagnetic systems changes in the electronic properties with dilution are small, but these are most marked where a phase transition occurs. In copper doped zinc complexes involving less rigid molecular complexes where the copper and zinc complexes are isomorphous, and for a range of stereochemistries, no change in structural or electronic properties is observed from 1—100% copper, which suggests that in these systems a non-cooperative Jahn-Teller effect is operating.

REFERENCES

1 W.E. Hatfield and R. Whyman, Transition Met. Chem., 5 (1969) 47.
2 B.J. Hathaway and D.E. Billing, Coord. Chem. Rev., 5 (1970) 143.
3 B.J. Hathaway and A.A.G. Tomlinson, Coord. Chem. Rev., 5 (1970) 1.
4 B.J. Hathaway and P.G. Hodgson, J. Inorg. Nucl. Chem., 35 (1973) 4071.
5 J. Gazo, I.B. Bersuker, J. Garaj, M. Kabesova, J. Kohout, H. Langerlderova, M. Melnik, M. Serator and F. Valach, Coord. Chem. Rev., 21 (1976) 253.
6 D.R. Eaton and K. Zaw, Coord. Chem. Rev., 7 (1971) 197.
7 J.S. Wood, Prog. Inorg. Chem., 16 (1972) 227.
8 B.J. Hathaway, Struct. Bonding, 14 (1973) 49.
9 B.J. Hathaway, Essays Chem., 2 (1971) 61.
10 D.W. Smith, Struct. Bonding, 12 (1972) 49; D.W. Smith, Coord. Chem. Rev., 21 (1976) 93.
11 Y. Nishida and S. Kida, Coord. Chem. Rev., 27 (1979) 275.
12 I. Bertini, D. Gatteschi and A. Scozzafava, Coord. Chem. Rev., 27 (1979) 67.
13 D. Reinen and C. Friebel, Struct. Bonding, 37 (1979) 1.
14 J. Pradilla-Sorzano and J.P. Fackler, Inorg. Chem., 12 (1973) 1182.
15 H.A. Jahn and E. Teller, Proc. Roy. Soc., 161 (1937) 220.
16 J.D. Dunitz and L.E. Orgel, J. Phys. Chem. Solids, 3 (1957) 20.
17 A. Abragam and B. Bleaney, Electron Paramagnetic Resonance of Transition Metal Ions, Clarendon Press, Oxford, 1970.
18 R. Englman, The Jahn-Teller Effect in Molecules and Crystals, Wiley, New York, 1972.
19 F.S. Ham, Phys. Rev., A, 138 (1965) 1727; 166 (1968) 307.
20 I.B. Bersuker, Coord. Chem. Rev., 14 (1975) 357.
21 S. Takagi, M.D. Joesten and P.G. Lenhert, Acta Crystallogr., Sect. B, 32 (1976) 326.
22 M.D. Joesten, M.S. Hussain and P.G. Lenhert, Inorg. Chem., 9 (1970) 151.
23 B.V. Harrowfield and J.R. Pilbrow, J. Phys., C, Solid State Phys., 6 (1973) 755; B.V. Harrowfield, Solid State Commun., 19 (1976) 983.
24 J.H. Ammeter, H.B. Burgi, E. Gamp, V. Meyer-Sandrin and W.P. Jensen, Inorg. Chem., 18 (1979) 733.
25 L. Cavalca, M. Nardelli and D. Grazioli, Gazz. Chim. Ital., 86 (1956) 1041; M. Van Driel and H.J. Verweel, Z. Kristallogr., 95 (1936) 308; D.L. Cullen and E.C. Lingafelter, Inorg. Chem., 10 (1971) 1264.
26 N.W. Isaacs and C.J.L. Kennard, J. Chem. Soc. A, (1969) 386.
27 M. Cola, G. Giuseppetti and F. Mazzi, Atti Accad. Sci. Torino, Cl. Sci. Fis., Mat. Nat., 96 (1962) 381; D.L. Cullen and E.C. Lingafelter, Inorg. Chem., 9 (1958) 1858.
28 M.D. Joesten, S. Takagi and P.G. Lenhert, Inorg. Chem., 16 (1977) 2680.
29 S. Takagi, M.D. Joesten and P.G. Lenhert, J. Am. Chem. Soc., 97 (1975) 444.
30 D. Mullen, G. Heger and D. Reinen, Solid State Commun., 17 (1975) 1249; S. Klein and D. Reinen, J. Solid State Chem., 25 (1978) 295; S. Klein and D. Reinen, J. Solid State Chem., 32 (1980) 311.
31 F.S. Stephens, J. Chem. Soc. A, (1969) 883.
32 A. Murphy, J. Mullane and B.J. Hathaway, Inorg. Nucl. Chem. Lett., 16 (1980) 129.
33 K. Knox, J. Chem. Phys., 30 (1959) 991.
34 H.G. Von Schnering, Z. Anorg. Allg. Chem., 353 (1967) 13.
35 I. Bertini, P. Dapporto, D. Gatteschi and A. Scozzafava, J. Chem. Soc., Dalton Trans., (1979) 1409.
36 A. Murphy and H.B. Burgi, private communication, 1979.
37 D.W. Phelps, D.B. Losee, W.E. Hatfield and D.J. Hodgson, Inorg. Chem., 15 (1976) 3147.

38 D. Reinen, C. Friebel and K.P. Reetz, J. Solid State Chem., 4 (1977) 103.
39 M. Duggan, A. Murphy and B.J. Hathaway, Inorg. Nucl. Chem. Lett., 15 (1979) 103.
40 C.K. Prout, R.A. Armstrong, J.R. Carruthers, J.G. Forrest, P. Murray-Rust and F.J.C. Rossotti, J. Chem. Soc. A, (1968) 2791.
41 L.L. Lohr, Inorg. Chem., 6 (1967) 1890.
42 H. Yamatera, Acta Chem. Scand., 33 (1979) 107.
43 D. Oerlkrug, Z. Phys. Chem. (Frankfurt am Main), 56 (1967) 325.
44 R.C. Koch, M.D. Joesten and J.H. Venable, J. Chem. Phys., 59 (1973) 6312.
45 N. Alcock, M. Duggan and B.J. Hathaway, unpublished results, 1979.
46 H.B. Burgi, private communication, 1979.
47 A. Murphy, Ph.D. thesis, University College, Cork, 1979.
48 S. Takagi, P.G. Lenhert and M.D. Joesten, J. Am. Chem. Soc., 96 (1974) 6606.
49 S. Takagi, M.D. Joesten and P.G. Lenhert, Acta Crystallogr., Sect. B, 32 (1976) 2524.
50 S. Takagi, M.D. Joesten and P.G. Lenhert, Acta Crystallogr., Sect. B, 31 (1975) 596.
51 H. Montgomery and E.C. Lingafelter, Acta Crystallogr., 20 (1966) 659.
52 G.M. Brown and R. Chibambaram, Acta Crystallogr., Sect. B, 25 (1969) 676.
53 D.J. Robinson and C.H.L. Kennard, Cryst. Struct. Commun., 1 (1972) 185.
54 J.J. Van Der Zee, K.G. Shields, A.J. Graham and C.H.L. Kennard, Cryst. Struct. Commun., 1 (1972) 367.
55 K.G. Shields and C.H.L. Kennard, Cryst. Struct. Commun., 1 (1972) 189; G. Smith, F.H. Moore and C.H.L. Kennard, Cryst. Struct. Commun., 4 (1975) 407.
56 N. Burger and H. Fuess, Solid State Commun., 34 (1980) 699.
57 B. Walsh, Ph.D. Thesis, University College, Cork, 1978.
58 N. Alcock, B. Walsh and B.J. Hathaway, unpublished results, 1979.
59 C. Friebel and D. Reinen, Z. Anorg. Allg. Chem., 407 (1974) 193.
60 C. Friebel, Z. Naturforsch., 296 (1974) 634.
61 M. Duggan, J. Mullane and B.J. Hathaway, J. Chem. Soc., Dalton Trans., (1976) 690.
62 A. Murphy, B.J. Hathaway and T.J. King, J. Chem. Soc., Dalton Trans., (1979) 1646.
63 Z.G. Soos, K.T. McGregor, T.T.P. Cheung and A.J. Silverstein, Phys. Rev. B, 16 (1977) 3036.
64 R.J. Dudley, B.J. Hathaway, P.G. Hodgson, P.C. Power and D.J. Loose, J. Chem. Soc. A, (1974) 1005.
65 N. Ray and B.J. Hathaway, J. Chem. Soc., Dalton Trans., (1980) 1105.
66 A. Bencini, I. Bertini, D. Gatteschi and A. Scozzafava, Inorg. Chem., 17 (1978) 3194.
67 M. Duggan, M. Horgan, J. Mullane, P.C. Power, N. Ray, A. Walsh and B.J. Hathaway, Inorg. Nucl. Chem. Lett., 16 (1980) 407 and references therein.
68 H. Elliott, B.J. Hathaway and R.C. Slade, Inorg. Chem., 5 (1966) 669.
69 B.J. Hathaway and R.G. Slade, J. Chem. Soc. A, (1968) 85.
70 C. Reinen, C. Friebel and K.P. Reetz, J. Solid State Chem., 4 (1972) 103.
71 B.J. Hathaway, P.G. Hodgson and P.C. Power, Inorg. Chem., 13 (1974) 2009.
72 R. Rajan and T.R. Reddy, J. Chem. Phys., 39 (1963) 1140.
73 I. Bertini, P. Dapporto, D. Gatteschi and A. Scozzafava, Solid State Commun., 26 (1978)749.
74 I. Bertini, D. Gatteschi and A. Scozzafava, Inorg. Chem., 16 (1977) 1973.
75 A.A.G. Tomlinson, Ph.D. Thesis, University of Essex, 1968.
76 P.C. Power, Ph.D. Thesis, University College, Cork, 1975.
77 I. Bertini and D. Gatteschi, Inorg. Nucl. Chem. Lett., 8 (1972) 207.
78 D.E. Billing, Inorg. Chim. Acta, 11 (1974) L31.
79 Van A.D.I. Schenau, G.C. Verschoor and C. Romers, Acta Crystallogr., Sect. B, 30 (1974) 1686.
80 D. Taylor, Aust. J. Chem., 31 (1978) 713.
81 T.J. Bergendahl and J.S. Wood, Inorg. Chem., 14 (1975) 338.
82 C.J. O'Connor and R.L. Carlin, Inorg. Chem., 14 (1975) 291.

83 D. Reinen and S. Krause, Solid State Commun., 29 (1979) 691; J.S. Wood, C.P. Keijzers, E. de Boer and A. Buttafava, Inorg. Chem., 19 (1980) 2213.
84 D. Reinen, Solid State Commun., 21 (1977) 173.
85 A. Walsh, Ph.D. Thesis, University College, Cork, 1976.
86 J. Pradilla-Sorzano and J.P. Fackler, Inorg. Chem., 12 (1973) 1174.
87 B.J. Hathaway, Autumn Meeting of the Chemical Society, Sheffield, Sept., 1976.
88 B.J. Hathaway, Electron Spin Resonance of Transition Metal Ions in Inorganic and Biological Systems, Nottingham, March 1979.
89 M.D. Joesten, S. Takagi and J.H. Venable, Chem. Phys. Lett., 36 (1975) 536.
90 B.J. Hathaway, M.J. Bew and D.E. Billing, J. Chem. Soc. A, (1970) 1090.
91 J. Mullane, Ph.D. Thesis, University College, Cork, 1976.
92 O.P. Anderson, J. Chem. Soc., Dalton Trans., (1972) 2597.
93 H.C. Allen, G.F. Kokoszka and R.G. Inskeep, J. Am. Chem. Soc., 86 (1964) 1023; G.F. Kokoszka, C.W. Reimann, H.C. Allen and G. Gordon, Inorg. Chem., 6 (1967) 1657.
94 F.E. Mabbs and J.K. Porter, J. Inorg. Nucl. Chem., 35 (1973) 3219.
95 M. Duggan, Ph.D. Thesis, University College, Cork, 1978.
96 F.S. Stephens, J. Chem. Soc. A, (1969) 2233.
97 A. Mathew and G.J. Palenik, J. Coord. Chem., 1 (1971) 243; R. Allmann, W. Henke and D. Reinen, Inorg. Chem., 17 (1978) 378.
98 Von W. Henke and D. Reinen, Z. Anorg. Allg. Chem., 436 (1977) 187.
99 M.A. Hitchman and T.D. Waite, Inorg. Chem., 15 (1976) 2155.
100 M.J. Bew, D.E. Billing, R.J. Dudley and B.J. Hathaway, J. Chem. Soc. A, (1970) 2640; K. Dawson, M.A. Hitchman, C.K. Prout and F.J.C. Rossotti, J. Chem. Soc., Dalton Trans., (1972) 1509.
101 B.L. Silver and D. Getz, J. Chem. Phys., 61 (1974) 638.
102 B. Nieuwenhuijse and J. Reedijk, Chem. Phys. Lett., 22 (1973) 201.
103 P.S. Rao and S. Subramanian, J. Magn. Resonance, 22 (1976) 191.
104 C. Sandmark and C.I. Branden, Acta Chem. Scand., 21 (1967) 993.
105 T.R. Reddy and R. Srinivasan, Phys. Lett., 22 (1966) 143; Proc. Indian Acad. Sci., 65 (1967) 303.
106 M. Narayana and G.S. Sastry, J. Phys. C, Solid State Phys., 12 (1979) 695.
107 B.J. Hathaway and B. Walsh, J. Chem. Soc., Dalton Trans., (1980) 681.
108 G.C. Shatz and J.A. McMillan, J. Chem. Phys., 55 (1971) 2342.
109 F. Murray, A. Murphy and B.J. Hathaway, unpublished results, 1979.
110 J. Chandrasekhar and S. Subramanian, J. Magn. Resonance, 16 (1974) 82.
111 G.L. McPherson and C.P. Anderson, Inorg. Chem., 13 (1974) 677.
112 D. Kennedy, M. Power and B.J. Hathaway, J. Chem. Soc., Dalton Trans., in press.
113 I.M. Procter, B.J. Hathaway, D.E. Billing, R.J. Dudley and P. Nicholls, J. Chem. Soc. A, (1969) 1192.
114 V.G. Krishnan, J. Phys. C, Solid State Phys., 11 (1978) 3493.
115 R.A. Palmer and C.R. Taylor, Inorg. Chem., 10 (1971) 2546.
116 B.J. Hathaway, R.J. Dudley and P. Nicholls, J. Chem. Soc. A, (1969) 1845.
117 B.J. Hathaway, M.J. Bew, D.E. Billing, R.D. Dudley and P.J. Nicholls, J. Chem. Soc. A, (1969) 2312.
118 R.M. Clay, J. Murray-Rust and P. Murray-Rust, Acta Crystallogr., Sect. B, 32 (1976) 111.
119 M.R. Lowrey and J.R. Pilbrow, J. Phys. C, Solid State Phys., 10 (1977) 439.
120 F. Hanic and A. Cakajdova, Acta Crystallogr., 11 (1958) 610.
121 J. Garaj, Chem. Commun., (1968) 904.
122 T.J. Greenough and M.F.C. Ladd, Acta Crystallogr., Sect. B, 34 (1978) 2744.
123 D.E. Billing, B.J. Hathaway and A.A.G. Tomlinson, J. Chem. Soc. A, (1971) 2839.
124 Z. Sroubek and K. Zdansky, J. Chem. Phys., 44 (1966) 3078.
125 S.H. Hagen and N.J. Trappeniers, Physica (Utrecht), 66 (1973) 166.

126 F. Boettcher and J.M. Spaeth, Phys. Status Solidi B, 61 (1974) 465.
127 N.J. Trappenier, F.S. Stibbe and J.L. Rao, Chem. Phys. Lett., 56 (1978) 10.
128 J.A.C. Van Ooijen, P.J. Van der Put and J. Reedjik, Chem. Phys. Lett., 51 (1977) 380.
129 D. Attanasio, G. Dessy and V. Fares, J. Chem. Soc., Dalton Trans., (1979) 28.
130 F.S. Stephens and I.M. Procter, J. Chem. Soc. A, (1969) 1248.
131 C.J. Simmons, M. Lundeen and K. Seff, Inorg. Chem., in press.
132 B.J. Hathaway, J. Chem. Soc., Dalton Trans., (1972) 1196.